Journal Pre-proofs

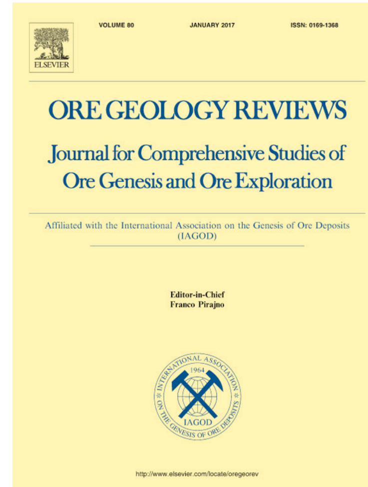

Mineral Chemistry And u-Pb Garnet Geochronology Of Strongly Reduced Tungsten Skarns At The Pampa de Olaen Mining District, Córdoba, Argentina

María José Espeche, Bo Wan, Raúl Lira, Reimar Seltmann

PII: S0169-1368(21)00405-4
DOI: https://doi.org/10.1016/j.oregeorev.2021.104379
Reference: OREGEO 104379

To appear in: *Ore Geology Reviews*

Received Date: 11 February 2021
Revised Date: 14 July 2021
Accepted Date: 22 July 2021

Please cite this article as: M. José Espeche, B. Wan, R. Lira, R. Seltmann, Mineral Chemistry And u-Pb Garnet Geochronology Of Strongly Reduced Tungsten Skarns At The Pampa de Olaen Mining District, Córdoba, Argentina, *Ore Geology Reviews* (2021), doi: https://doi.org/10.1016/j.oregeorev.2021.104379

MINERAL CHEMISTRY AND U-Pb GARNET GEOCHRONOLOGY OF STRONGLY REDUCED TUNGSTEN SKARNS AT THE PAMPA DE OLAEN MINING DISTRICT, CÓRDOBA, ARGENTINA

María José ESPECHE[1,2]*, Bo WAN[3], Raúl LIRA[1,2] and Reimar SELTMANN[4]

[1]Laboratorio de Microscopía Óptica y Microtermometría – Museo de Mineralogía y Geología "Dr. Alfred W. Stelzner" – Facultad de Ciencias Exactas, Físicas y Naturales, Universidad Nacional de Córdoba. Av. Vélez Sarsfield 299, X5000JJC, Córdoba, Argentina.

[2]Consejo Nacional de Investigaciones Científicas y Técnicas (CONICET), Córdoba, Argentina.

[3]State Key Laboratory of Lithospheric Evolution, Institute of Geology and Geophysics, Chinese Academy of Sciences, Beijing, 100029, China.

[4]Center for Russian and Central Eurasian Mineral Studies, Department of Earth Sciences, Natural History Museum, London, UK.

*corresponding author: majo.espeche@unc.edu.ar

ABSTRACT

Los Guindos scheelite (± Zn, Bi, Sn, Ag) skarn presents mineral assemblages and a mineral chemistry similar to other worldwide strongly reduced W skarn deposits. Its reduced nature is defined based on the predominance of subcalcic garnets, Mo-free scheelite and absence of magnetite. Both the prograde and retrograde stages are evident at Los Guindos scheelite skarn. The prograde skarn is characterized by three zones: A zone I of garnet + helvine ($Gr_{57}Sp_{24}Ad_{19}Alm_8$ - $Sp_{50}Alm_{24}Gr_{22}Ad_3$; Grt + Hlv); a zone (II) of clinopyroxene + garnet ($Di_{67}Hd_{24}Jo_9$ + $Gr_{66}Sp_{19}Ad_{12}Alm_3$; Cpx + Grt) and a zone (III) of garnet + vesuvianite ($Gr_{73}Ad_{22}Sp_3Alm_2$ - $Gr_{58}Sp_{22}Ad_{10}Alm_9$; Grt + Ves). Retrograde skarn is mainly represented by epidote - actinolite and minor F-rich actinolite (0.663 apfu of F) – potassium feldspar - chlorite (chamosite/clinochlore: ~ 50/50) – muscovite – calcite - quartz. A hydrothermal stage developed in temporal continuity with retrograde skarn formed variable infilling associations of the following species: epidote – actinolite – scheelite – fluorite – calcite – quartz – sphalerite and chlorite. Scheelite mineralization process was triggered by an increase of Ca released during retrograde skarn replacements and was deposited during the following hydrothermal infilling stage. Other than sphalerite, minor bismuthinite and tetradymite, andorite, lillianite, gustavite, matildite and kësterite occur as hydrothermal associations after scheelite deposition. Scheelite-free reaction skarn preceding scheelite skarns was observed. Geobarometric calculations in this reaction skarn suggests an initial confining pressure of 2.5 kbar for the Los Guindos scheelite skarns. This pressure matches the estimated emplacement pressure of the Devonian-Carboniferous Achala batholith reported by previous authors. Geochemical correlation analyses suggest that this magmatism may have contributed mineralizing fluids channeled through regional structures and lithological contacts, causing infiltration metasomatism that originated scheelite (± Zn, Bi, Sn, Ag) mineralization in Cambrian and Ordovician country rocks. U-Pb analyses (LA-ICP-MS) of

garnet in the Los Guindos scheelite skarn gave an age of 361 ± 11 Ma representing the age of the prograde stage of scheelite skarns and it should be framed within the Devonian-Carboniferous Metallogenic Epoch.

Keywords: Garnet U-Pb age, U-Pb geochronology, garnet/pyroxene chemistry, scheelite skarn, Achalian magmatism, Córdoba Ranges.

1. INTRODUCTION

The Eastern Pampean Ranges of Córdoba province host numerous tungsten deposits of different types and sizes, a fact that prompted Angelelli (1984) to group them into a Wolframiferous Metallogenetic Province. The scheelite deposits registered in the Sierras de Córdoba basement are those studied in Altautina (Ametrano, 1999), Ambul (Herrmann, 2002), El Zinqui mine (Skirrow, 1997) and Los Guindos mining group (LGMG, Pampa de Olaen Mining District; Valdez, 1984; Espeche and Lira, 2018; Fig. 1). However, scheelite (± wolframite) occurrences related to hydrothermal remobilization farther extends to the south into the San Luis province (Sierra del Morro Oeste-Este, Sierra de Yulto, Libertador General San Martín, La Estanzuela and Villa Praga Districts; de Brodtkorb and Brodtkorb, 1999; Brodtkorb et al., 1999; Etcheverry and Brodtkorb, 1999; Montenegro et al*.,* 2009; Galliski et al., 2019; Enriquez et al., 2019). Quartz-wolframite (± scheelite) greisen-related vein deposits are also found in Córdoba province like in Cerro Áspero (Fernández Lima et al., 1963; Coniglio et al., 2000; Mutti and González Chiozza, 2005), Agua de Ramón (Lapidus and Rossi, 1959; Tourn, 1999; Skirrow et al., 2000; Biglia et al., 2016), Capilla del Monte (Massabie, 1982; Agulleiro Insúa et al., 2013) and Mesa de Mula Muerta (Monsberger, 1990). Despite the numerous tunsgsten deposits and ocurrences present within the Eastern Pampean Ranges, there are few studies referring to the origin, dynamics and evolution of hydrothermal fluids, and studies of some of these deposits, deemed as scheelite skarns, are even less (Espeche and Lira, 2018, 2019a). This contribution presents the geology, classification, mineral chemistry and geochronological data of the Los Guindos scheelite skarn. Its mineral chemistry and most outstanding features are compared with the most currently accepted classification of skarn deposits and with other W skarn deposits of the world. The U-Pb age of garnet skarn corresponds to the first record of an absolute age for a metasomatic event in Córdoba Ranges.

2. GEOLOGICAL SETTING

The evolution of the Córdoba Ranges forms part of larger events occurred in the South American Platform, during the Neoproterozoic-Lower Paleozoic. The Córdoba Ranges are composed of four major ranges of meridian orientation named Sierras de Guasapampa, Pocho and Altautina, Sierra Grande and its southernmost extension as Sierra de Comechingones, Sierra Chica and Sierra Norte. They are made up of Neoproterozoic to Cambrian metamorphic rocks intruded by Paleozoic granitoids that underlie small Carboniferous-Permian and larger Cretaceous and Cenozoic intermountain continental sedimentary basins (Gordillo and Lencinas, 1979; Astini and del Papa, 2014; Astini and Oviedo, 2014; Astini et al., 2014; Carignano, 2014). To the west sector trachyandesitic volcanic necks and pyroclastic deposits of Neogen age emerge spread over the east-tilted basement ranges (Gordillo and Lencinas, 1979; Kay and Gordillo, 1994; Fig. 1). The lithological constitution of the Córdoba Ranges is largely composed of Late Ediacaran-Early Cambrian metamorphic rocks composed of phyllites, schists, gneisses, ultramafic and mafic rocks, marbles, amphibolites and migmatites, varying the metamorphic grade from greenschist facies in the west (Sierra de Pocho) to high grade orthogneisses and migmatization to the northwestern in isolated domains of the San Carlos Massif and central-eastern region (Sierra Grande and Sierra Chica ranges; Guereschi and Martino, 2014, and references therein). Voluminous intrusive magmatic activity since Cambrian times (Pampean Orogeny, 540 to 515 Ma), through the Early-Middle Ordovician (Famatinian Orogeny, 478–460 Ma) until the Upper Devonian to Lower Carboniferous (Achalian magmatism, 413-336 Ma; Dorais et al., 1997; Dahlquist et al., 2013a; D'Eramo, 2014; Galliski and Sfragulla, 2014; Lira and Sfragulla 2014; Pinotti, 2014) are recorded in Córdoba Ranges. These metamorphic-igneous complexes are made up of a series of lithological – structural domains separated by ductile shear zones (Martino and Guereschi, 2014).

Of the three periods of magmatic activity, the most important from a metallogenetic point of view is doubtless the Achalian magmatism (Rapela, 1982; Lira and Kirschbaum, 1990; Rapela et al., 2008; Lira and Sfragulla, 2014). The greatest expressions of this magmatism are represented by the Achala Batholith (2,500 km^2) followed by the Cerro Áspero Batholith (660 km^2) and small (4-80 km^2) ellipsoidal plutons peripherical to the Achala Batholith which share age, similar geochemical signature and geotectonic setting (Fig. 1). The Achala granites were classified as of the A-type magmatism, aluminous to peraluminous, calc-alkaline to alkali-calcium granites of Devonian-Carboniferous age (Galliski, 1993, 1994; Dorais et al., 1997; Rapela et al., 2008; Dahlquist et al., 2013a, 2013b). Geochemical data show low contents of Ca, Mg, Fe, Ti, Zr, Ba and Sr, and relatively high contents of Si, Na, K, Rb, Nb, low K/Rb ratio and very high Rb/Sr ratio, indicative of strong magmatic differentiation and fractionation, mostly explained by fractional crystallization (Lira and Sfragulla, 2014; Morales Cámera et al., 2020).

Economic interest has been placed in this magmatic event, given its high content of incompatible elements and the well-developed fractionation processes that conditioned its high specialized nature and favored the formation of Be-Nb-Ta-P- rich intra- and peri-batholithic pegmatites (Hybrid-NYF family, Galliski and Sfragulla, 2014) and hydrothermal F-rich processes with often associated mineralizations of hydrothermal - supergene U deposits, Au-Pb-Ag-Zn mesothermal veins and W and W-Bi metasomatic deposits (Fig. 1, Lira et al., 1996; Coniglio et al., 2000; Skirrow et al., 2000; Herrmann and Tourn, 2002; Mutti and Gonzalez Chiozza, 2005; Blasón et al., 2014; de Brodtkorb et al., 2014; González Chiozza, 2021). Its high F content, evidenced not only in accesory magmatic minerals (biotite-fluorapatite, Demange et al., 1996; Dorais et al., 1997), but also as fluorite-rich greisen and skarns (Lira et al., 1996; Franchini and Lira, 1998), and fluorite epithermal veins related to extensional tectonic regime of Cretaceous age (Rimann, 1918; Galindo et al., 1996; Bonalumi et al., 1999a; Coniglio et al., 2000) are characteristic of this magmatism.

Nevertheless, besides all studies made to these deposits that prove the genetic link with the Achala magmatism, there are no whole rock analyses that show the enrichment (or not) of W and other metals incompatible with adequate techniques, even that bulk tungsten enrichment in associated granitoids does not appear to be a requirement to the formation of scheelite skarn (Newberry and Swanson, 1986). On the basis of geochronological data of gangue minerals associated to different Pb-Ag-Zn, Au-Ag-Cu epi-mesothermal vein deposits and W greisen, Skirrow et al. (2000) collectively grouped those into a “Devonian Metallogenic Epoch”, spanned from ~ 390 to 360 Ma. Farther north, in the Sierra de Sumampa, carbonatite LREE (Nb) mineralization is also geochronologically related to the Devonian Metallogenic Epoch (Fig. 1, Franchini et al., 2005). However, there is a transition of some of these deposits into the Carboniferous age, as the NYF or mixed NYF-LCT signature) intragranitic pegmatites of the batholith, which yielded biotite and muscovite K/Ar cooling ages between 356 ± 10, 350 ± 30 and 352 ± 25 Ma (Linares and Latorre, 1969; Linares and Kleiner, 1973). These ages would represent part of the dawning of the Achalian magmatic cycle and the so called “Devonian Metallogenic Epoch” since the systems continued and ended into Carboniferous times.

3. MINING HISTORY AND LOCAL GEOLOGY OF LOS GUINDOS MINING GROUP

3.1. MINING HISTORY

Los Guindos mining group is located in the Punilla department, Córdoba province, covering an area of ~ 13 km^2 on the central-eastern zone of the Sierra Grande de Córdoba, west of the Punilla valley. It is limited to the west by the easternmost expressions of the Achala Batholith and to the east by the NW-SE Matacaballos Shear Zone (Fig. 1) where numerous strongly altered ultramafic rock bodies emerge in lengths up to 240 m and 105 m wide, with variable N 300–340° strike and 60° SW dip (Cuervo, 1988; Bonalumi et al., 1999b).

During the first half of the 20th century, Los Guindos mining group was one of the main producers of scheelite in Córdoba province, mainly since the 40's to the early 60's. There are numerous private and state companies, and academic reports of economic-mining attributes made since 1954 until 1984, among others Oliveri (1954, 1957), Lucero (1956), Holmberg (1960), Llambías (1963), Pezzutti (1982) and Valdez (1984). From 1943 to 1963, the exploitation of about 15 mines was carried out by the Olaen Mining and Industrial Society (SOMINOL) through small surface mining operations and, in the case of the Mogote de la Picaza mine, underground through rudimentary galleries. From 1943 to 1963 ~ 200 t of concentrates (69.22 % WO_3) were produced. In 1963 the exploitation was paralyzed due to the collapse of cost-effective processes (Valdez, 1984) and any further systematic exploration work in the district has been developed since then, hence, at present, any reserve or resource estimation is available.

3.2. LOCAL GEOLOGY

The basement of the study area is composed, in order of outcropping abundance, of sillimanite gneisses, biotite-garnet gneisses, stromatitic migmatites, marbles, amphibolites, pegmatite dikes, tonalitic-granodioritic orthogneisses, medium and fine-grained tonalitic dikes, hornblendites, alkali-feldspathic granite dykes and microgranite dikes. The entire sequence comprises the Upper Proterozoic – Lower Cambrian basement denominated by Demange et al. (1993) as Iggam Group, which resulted from metamorphic and deformational processes mainly related to the Pampean Orogeny. The orientation of foliation of metamorphites in the region shows a complex deformational history, with superposition of compressive and shearing metamorphic events in a ductile and fragile environment. The general orientation of foliation is ~ NE-NW with a west-predominant high dip angle (~ 70 - 50°). A few granitoids of Ordovician and Devonian-Carboniferous age related to the Famatinian Orogeny and Achalian magmatism, respectively, are present in the area; the former as small tonalitic and granodioritic dikes that crosscut the marbles and formed small and barren skarns; the Achalian event is represented as undeformed microgranite dikes, of less than 2 m width and a few meters of continuous length that cut with low angle the foliation of the metamorphic basement; the nearest representative facies of the Achala batholith, i.e., the coarse-grained porphyric facies, is widely exposed ~1.5 km west of the scheelite skarn outcrops. Field evidence shows that scheelite skarns are not genetically related to Ordovician granitoids; they are found distally from Ordovician granitoids and these are notably deformed in structural concordance with the Cambrian-Ordovician foliation. Scheelite skarn bodies are not deformed; they developed as small to medium sized, irregular shaped bodies of a few to a few hundreds of square meters area. The field correlation of tens of points of these bodies in the studied area shows that these rocks present an irregular morphology (Fig. 2). Grassy and bushy vegetation makes it difficult to map the numerous skarn bodies spread throughout the mining group region, though differential weathering, topographic highs (quartz rich zones) and abandoned mining works, make it possible to distinguish these bodies from other country rock lithologies. Preceding the formation of scheelite skarns there are also some scheelite-free reaction skarns of reduced dimensions in close spatial association with W-mineralized skarns.

3.2.1. BARREN SKARNS RELATED TO TONALITIC, GRANODIORITIC AND GRANITIC APLITE-PEGMATITE DIKES

Barren skarns related to Ordovician mesosiliceous granitoids are less than 10 cm wide and are composed of thin bands of mainly clinozoisite, epidote, garnet, plagioclase and titanite, among other minor species. Some Ordovician granitic aplite-pegmatites also present as small bands (< 10 cm wide) of dominating pink clinozoisite (garnet - clinopyroxene - amphibole - epidote - scapolite – quartz – calcite – apatite - titanite) at the contact with calcic marbles, resulted from low scale metasomatic processes. Practically identical skarn mineral associations, with the remarkable presence of coarse-grained blue scapolite and titanite, were described by Lira and Gay (1999) between aplite-pegmatite Ordovician deformed dikes and marbles along the eastern border of Pampa de Olaen, in the San Antonio marble quarries (S 31° 06’ 52” – W 64° 30’ 15”).

3.2.2. SCHEELITE-FREE REACTION SKARNS

Scheelite-free reaction skarns are also found at Los Guindos Mining District though not as common as skarns related to the Ordovician granitoid dikes. These reaction skarns form small (10-20 m^2), fine grained bodies, poorly developed in calcic marbles and normally associated with the scheelite skarns.

The characteristic mineral association of one of these scheelite-free reaction skarns is dominated by clinopyroxene, garnet and titanite. Two retrograde associations are recognized: 1- epidote as subhedral and euhedral crystals of 2-4 mm long and 2- actinolite and chlorite as replacement of pyroxene and epidote. Calcite and quartz make up the filling phase along with sphalerite 1 (Sp 1), chalcopyrite, pyrrhotite and pyrite. Reaction skarn is found as few meters sized remnant lenses of dominantly pale green color, embedded in coarse grained scheelite skarn (crystals up to several centimeters long) composed of garnet, vesuvianite, epidote, clinozoisite and thick lenses of infilling quartz (Fig. 3). In the contact of some quartz lenses with this reaction skarn and the latter coarse-grained scheelite skarn, aggregates of sphalerite 2 (Sp 2, up to 10 cm wide) and/or iron-rich hydrothermal carbonates are usually found.

The reaction skarn does not present zonation or textural variations along the major extension or width of the outcrops, neither surface with centimetric development of crystals or large aggregates of infilling calcite or quartz have been observed; rather, the reaction skarn is homogeneous and, in some sectors, it presents a slight banding that appears to be inherited from the replaced marble (Fig. 3). Geobarometric estimates based on FeS mole %

(Hutchison and Scott, 1981) in infilled sphalerite 1 associated with chalcopyrite, pyrrhotite and pyrite revealed formation pressure conditions of these pre-ore skarns of ~ 2.5 kbar.

3.2.3. MINERALOGY AND ZONING OF SCHEELITE-BEARING SKARNS

Los Guindos scheelite skarn bodies were preferentially developed after the replacement of marbles and have a characteristic repetitive zonation in all outcrops, although some zones can be much more reduced in size than others or be absent, probable due to local variations on the composition of the metasedimentary protholith (country rocks) in each outcrop.

3.2.3.1. PROGRADE SKARN

The zonation of prograde associations is characterized, from the source of incoming fluid (considered as N-NW strike and W-SW dip faults developed at the contact between granitic aplite-pegmatite dikes and marble) towards the marble, by a zone (I) of garnet ± helvine, a zone (II) of clinopyroxene ± garnet and a zone (III) of garnet + vesuvianite (Fig. 4a, b, c, d). Recrystallized marbles were recognized a couple of meters far away from the skarn outcrops. In some outcrops where the skarn was formed replacing aplite-pegmatite dikes, is common to find 10 to 20 cm wide voids lined with centimeter-sized, idiomorphic prismatic plagioclase crystals (e.g., Loma Pajosa and Chingolo mines, Figs. 4). Prograde associations are developed as projections of crystals in cavities forming druses; many are rooted as polycrystalline anhedral massive aggregates and others are perfect free idiomorphic individual crystals that might be partially or totally covered by some of the late infilling minerals; the crystal growth continuity from massive aggregates to free idiomorphic crystals is generally observed. Prograde skarn zones II and III host disseminated and scarce scheelite where both zones have been strongly overprinted by retrograde skarn mineral associations, while higher concentrations of scheelite are found where the same zones have been infilled by late hydrothermal minerals.

3.2.3.1.1. ZONE I

Zone I is composed mainly of aggregates of euhedral garnet crystals of up to 1 cm in size (Fig. 5a), of a dark red translucent color; this area is developed from the replacement of aplite-pegmatite dikes. In the dumps of El Minerito mine, Valdez (1984) describes the presence of helvine crystals filling drusic cavities associated with garnet and quartz which clearly belong to this zone; in this mine, the zone 1 is partially affected by a post-skarn fault zone that promoted strong alteration and masked the skarn assemblage with low temperature hydrothermal and/or supergene clay minerals and Zn-Fe rich oxides. Nevertheless, the presence of helvine in zone I is not as abundant as in Chingolo mine and only a few crystals were found; instead, radial aggregates of aquamarine beryl crystals of 2 mm up to 1 cm in length are common (Fig. 5b).

3.2.3.1.2. ZONE II

It is defined by the clinopyroxene ± garnet association (Fig. 5c). The skarn in this zone is banded; the mineral association is arranged in bands less than 1 cm wide of clinopyroxene (± garnet). In those marbles that present interbedded amphibolite lenses, being common in Los Guindos, the formation of the skarn is restricted only to marble, leaving the amphibolite lenses as unaltered relics immersed in the mass of the skarn, except for their edges that have been partially replaced by the retrograde epidote-actinolite-chlorite association. Optically, clinopyroxene is euhedral, pale green in color and occurs in crystals that do not exceed 2 mm long. Crystals are strongly altered by actinolite, potassium feldspar, epidote and less chlorite (Fig. 5c, d). Although garnet is scarcer than clinopyroxene, it develops in crystals of larger size than the latter and partially includes it in some sectors. The crystals are dark red euhedral, from 1 mm to 2 cm in size and anisotropic. Fluorapatite is an abundant accessory in this zone; it is found in sub-rounded to rounded euhedral crystals up to 0.5 mm in size included in the matrix of fluorite or in contact with the replaced crystals of clinopyroxene and garnet. Titanite is very scarce and occurs as euhedral crystals of up to 0.25 mm isolated and uniformly distributed in the filling matrix or associated, like apatite, with clinopyroxene and / or garnet replaced by retrograde mineral assemblages.

3.2.3.1.3. ZONE III

This zone is composed of the association Grt - Ves - Cpx - Ap. Garnet crystals are euhedral ranging from 100 μm to ~ 10 centimeter in size. Some garnet crystal faces are covered by fluorite filling that also envelops prismatic vesuvianite crystals. The latter is found in prismatic euhedral crystals from 1 cm to approximately 10 cm of length that include smaller euhedral crystals of clinopyroxene strongly replaced by actinolite and intensely fractured with epidote filling (Fig. 5f, g). Apatite is very abundant in this zone; it is found as euhedral crystals of up to 100 μm included in vesuvianite.

3.2.3.2. RETROGRADE SKARN

The retrograde skarn associations are composed of epidote - amphibole (actinolite and F-rich actinolite) - potassium feldspar - chlorite (chamosite / clinochlore: ~50/50) – calcite – muscovite (sericite) – quartz, which distribution and abundance are controlled by the proper mineralogy of each prograde zone. In zone I, epidote, potassium feldspar, bertrandite (Fig. 4e, f), chlorite and muscovite dominate as retrograde associations; in zone II, chlorite, calcite and quartz replaced garnet while actinolite, potassium feldspar and lesser epidote and chlorite replaced clinopyroxene; in zone III, alteration is dominated by scarce calcite and epidote replacing garnet.

3.2.3.3. SCHEELITE MINERALIZATION STAGE

Tungsten mineralization is characterized by Mo-free scheelite deposition mainly in zone II and to a lesser extent in zone III as bands or lenses included mostly in fluorite. It is also noticed in some skarn bodies that many aggregates of epidote, actinolite, and scheelite finish off in idiomorphic crystals within cavities filled with spar calcite, quartz and/or fluorite, indicating areas of primary high porosity during skarn formation in zones II and III. Textural relations between retrograde skarn associations and scheelite infilling lenses, bands or patches show a spatial and temporal continuity between both stages, where scheelite-calcite-fluorite-quartz likely represent hydrothermal fluids related to the final stages of retrograde alteration.

The most abundant sulfide associated with post-scheelite phases is Fe-bearing sphalerite, with its major development in zone II (Fig. 4), although it is common to find bismuthinite and less frequently tetradymite, andorite, lillianite, gustavite, kësterite, matildite and secondary products (i.e., kettnerite) randomly distributed though scarcely found (Gamba, 1996; Sureda et al., 2006). Fluorite, calcite, chlorite (chamosite / clinochlore: ~50/50) and quartz constitute the main post-ore hydrothermal filling phases in zones I to III. Minor species as hemimorphite and Zn-rich pyrophanite (Espeche and Lira, 2020) were found associated with infilling chlorite and calcite in zone I. Even some infilling minerals are found in retrograde skarn, they can be differentiated; for example, at least three generations of calcite were recognized: retrograde calcite formed by the pseudomorphic replacement of garnet, called "Cal_1" in Fig. 5g; fluorescent (pink colored) infilling spar calcite (some rhombohedra may exceed 5 cm in length) associated to scheelite and quartz (e.g. in Mogote de la Picaza mine), called "Cal_2"; and calcite in thin veins crossing the prograde and infilling associations defined as "Cal_3".

3.2.3.4. SUPERGENIC STAGE

Supergenic mineral associations include fraipontite, hemimorphite, calcite, kettnerite, bismuthite and Fe oxides-hydroxides. A schematic simplified representation of all the zones of Los Guindos scheelite skarn is depicted in figures 7 and 8.

3.2.4. SCHEELITE-FREE SKARNS

In Los Guindos mining group, there are also some small barren skarn bodies heterogeneously distributed in the same area of the scheelite-bearing skarns. These barren skarns were particularly formed after the partial replacement of pegmatites and amphibolites, characterized by Ca-rich garnet ($Gr_{81}Ad_{17}Sp_{1.5}Alm_{0.5}$, Espeche et al., 2019b) + clinopyroxene ($Di_{83}Hd_{16}Jo_{1}$, Fig. 4h), massive aggregates of epidote + quartz (Fig. 4i); and garnet skarn (± clinopyroxene, $Gr_{61}Ad_{24}Sp_{12}Alm_{3}$ ± $Di_{60}Hd_{34}Jo_{6}$) strongly affected by a gossan-like alteration zone rich in secondary Fe-Cu oxidation minerals (Fig. 4j). In the latter, it is assumed that the secondary Cu-bearing minerals and the Fe-oxides/hydroxides derive from the oxidation of accessory phases such as chalcopyrite, pyrite and magnetite from amphibolites. The main difference between scheelite-mineralized and scheelite-free skarns consists in the nature and composition of the replaced country rock; scheelite is hosted in replaced marbles and is not found in replaced aplite-pegmatite bodies (prograde skarn of zone 1) neither in replaced amphibolites. A general observation valid for the whole district is that the degree of skarn replacement of the three most reactive country rocks is marble>>amphibolite>aplite-pegmatite.

METHODOLOGY

3.3. QUANTITATIVE ANALYSES

Electron probe microanalyzer (EPMA) analyses of garnet (n= 95) and pyroxene (n= 117) from Los Guindos scheelite skarn (zones I to III) and from scheelite-free reaction skarn (n= 21 in garnet and n= 15 in clinopyroxene) of different outcrops were carried out with a Jeol JXA 8230 electron microprobe in wavelength dispersive mode (WDS), located in the Laboratory for Electron Microscopy and X-Ray Analyses (LAMARX), at the Faculty of Mathematics, Astronomy, Physics and Computing of the Córdoba National University, Argentina. Garnet and pyroxene were classified according to the approved IMA criteria of Grew et al. (2013) and Morimoto et al. (1988), respectively. Mineral name abbreviations are according to Whitney and Evans (2010). Since the majority of the analyzed garnet has high F contents, the calculation of the structural formula has been carried out considering the possible substitutions and tetrahedral vacancies at the structural sites; hence, normalization was carried out based on 5 cations ($X + Y$) and the calculation of Fe^{+3} was carried out as a function of the cationic deficit at the octahedral site Y considering all the Al and Ti at this site (Fe^{+3} = 2-[Al+Ti]; Fe+2X = Fe_{total}-Fe^{+3}). This criterion was chosen assuming that there is no substitution of Si at the tetrahedral site for Al or Ti, in order to be able to calculate the tetrahedral vacancies, OH and F from the substitution reaction of Valley et al. (1983). The equipment measurement conditions for the garnet group minerals were 20 nA (Mg, Si, W, Mn, Fe, Ti, Ca, Sn and Zn) and 10 nA (F, Al, Cl, Cu and Mo) of beam current, potential of 15 Kv, beam diameter of 5 µm, 10 seconds of counting at the peak and 5 seconds at the bottom, except for the W, Sn, Cu, Zn and Mo in which was applied 20 s in the peak and 10 s in the background. The standards used were the following: topaz (F), olivine_forsterite (Mg, Si), anorthoclase (Al), $CaWO_4$ (Ca, W), sodalite (Cl), rhodonite (Mn), ilmenite (Ti, Fe), cassiterite (Sn), cuprite (Cu), ZnO (Zn) and wulfenite (Mo).

The measurement conditions for pyroxene (clinopyroxene) were 20 nA (Mg, Si, Mn, Fe, Ti, Ca, Cu and Zn) and 10 nA (F, Al) of beam current, potential of 15 Kv, beam diameter of 3 µm, 10 s of counting at the peak and 5 s in the background, except for Cu and Zn for which were applied 20 s at the peak and 10 in the background. The standards used were the following: topaz (F), olivine_forsterite (Mg, Si), anorthoclase (Al), wollastonite (Ca), rhodonite (Mn), ilmenite (Ti, Fe), chalcopyrite (Cu), chromite (Cr) and sphalerite (Zn).

3.4. U-Pb GEOCHRONOLOGY

Isotopic measurements were carried out in an Agilent 7500a (Agilent Technologies, Japan) mass spectrometer coupled with an excimer 193 nm laser ablation system at the Institute of Geology and Geophysics, Chinese Academy of Sciences (IGGCAS). Detailed analytical procedures and experimental parameters are described by Yang et al. (2018), which were successfully applied to a skarn ore deposits in China (Zang et al., 2019). Standards were two matrix-matched external references andradite (Willsboro and Magana Mali) and one internal standard NIST 612 glass. Ratios of $^{207}Pb/^{206}Pb$ and $^{206}Pb/^{238}U$ were calculated using GLITTER 4.0. Data reduction was carried out using the IsoplotR program (Vermeesch, 2018).

4. RESULTS

4.1. MINERAL CHEMISTRY OF SCHEELITE SKARNS

4.1.1. GARNET

As it is shown in figure 8, garnet compositions vary from the prograde zones I to III, from subcalcic-rich member garnets, being the subcalcic component characterized mainly of spessartine in zone I within a range of $Sp_{59}Alm_{23}Gr_{17}Ad_1$ - $Gr_{59}Sp_{23}Ad_9Alm_9$, while in zone II the range varies from $Gr_{79}Ad_{18}Sp_2Alm_1$ to $Gr_{53}Sp_{25}Ad_{19}Alm_3$ and in zone III varies from $Gr_{89}Ad_7Sp_2Alm_2$ to $Gr_{46}Sp_{25}Alm_{15}Ad_{14}$. Some garnet analyses have high OH and F content (> 0.5 apfu in ϕ site) and can be named as fluoro- and hydroxi- grossular, respectively. Because the zone I is mostly developed after replacement of an aplite-pegmatite dike, and zones II and III mainly formed after the replacement of calcite marbles (Fig. 4a, b), the transition from zone I to zones II and III is abrupt. An intracrystalline zonation is also recorded from core to rim from calcic-rich member (mainly grossular) with low subcalcic composition (spessartine) to spessartine-dominant composition (Fig. 9). Almandine and andradite members do not show a representative variation in any of the prograde zones and crystals; however, it is noticed that andradite compositions vary proportionally with grossular contents whereas almandine reflects the same variation with respect to spessartine. Microprobe analyses in almost all crystals from zone I to III show considerable F^- content ($\bar{x}$ = 0.55 % F^-, n = 95) with a maximum of 1.36 % of F^- analyzed in zone III and a minimum of 0.02 % in zone I. The OH^- calculated has an average of 0.69 % (as H_2O content for n = 95).

4.1.2. CLINOPYROXENE

Clinopyroxene grains of zone II present oscillatory zonation from core to rim due to the compositional variation of $Mg^{+2}/(Fe^{+2} + Mn^{+2})$, reflected in a slight but clear variation of the molar proportions of diopside *vs* hedenbergite + johannsenite. The range of compositions is comprised in all the crystals between $Di_{76}Hd_{19}Jo_5$ and $Di_{55}Hd_{31}Jo_{14}$. The ZnO content does not exceed 0.34 wt. %. Nevertheless, clinopyroxene from the prograde zone III is very scarce; it is found as subhedral inclusions of up to 200 µm in vesuvianite and / or garnet and is strongly replaced by fibrous amphiboles of the tremolite-actinolite series. Clinopyroxenes show no compositional zoning; and are immersed in an interstitial epidote aggregate. The composition of clinopyroxene in this zone is richer in Mg (diopsidic) than that analyzed in the prograde zone II. Molar compositions range from $Di_{83}Hd_{14}Jo_3$ to $Di_{63}Hd_{30}Jo_7$. The average ZnO content is 0.33 wt. %.

4.2. MINERAL CHEMISTRY OF SCHEELITE-FREE REACTION SKARN

4.2.1. GARNET

Garnet of the scheelite-free reaction skarn presents oscillatory zonation from core to rim although the composition does not present a marked contrasting variation. The molar proportion ranges from $Gr_{51}Sp_{21}Alm_{18}Ad_{10}$ in the core to $Gr_{58}Sp_{17}Alm_{13}Ad_{12}$ in the rim. The maximum F content of the analyzed crystals is 0.38 wt. % and they do not present appreciable ZnO.

CLINOPYROXENE

Clinopyroxene analyses of scheelite-free reaction skarn show differences with those of pyroxenes of the scheelite skarn zones (Table 2, figure 8). Clinopyroxenes of the scheelite-free reaction skarn show a distinct trend with an enrichment of Fe (Table 1, figure 8). They have a mean molar composition of $Di_{48}Hd_{46}Jo_6$; zonation follows the same pattern, where the compositional variation is due to changes in the $Mg^{+2}/(Fe^{+2} + Mn^{+2})$ ratio, decreasing slightly from core to rim in all the analyzed crystals. The ZnO content does not exceed 0.14 wt. %.

4.3. U-Pb GEOCHRONOLOGY

The garnet crystals chosen for U-Pb geochronology were sampled at the Chingolo mine (Fig. 2). Chingolo mine is one of several mining works which belongs to LGMG. It is an abandoned small scheelite mine, where a 5 m wide skarn formed in the contact of an Ordovician pegmatite with marble along an extension of tens of meters parallel to the marble-pegmatite contact. The analyzed garnet crystal corresponds to the garnet + helvine prograde zone, closer to the pegmatite body. Garnet is found in masses of euhedral crystals of up to 2 cm in edge size. They are dark with a translucent reddish tone which crystallized in the dominant form {211} (Fig. 11). Microprobe analyses show spessartine compositions varying from $Sp_{76}Ad_{24}$ to $Sp_{55}Ad_{22}Gr_{23}$ from core to rim. Twenty-three U-Pb spot analyses were placed on selected regions. The measured $^{206}Pb/^{238}U$ ratios gave an age of 361.0 ± 11.0 Ma (MSWD = 0.026; n = 23; table 8). The weighted average gave an mean error of 0.0572 ± 0.0010, with a 95% confidence.

5. DISCUSSION

5.1. SKARN CLASSIFICATION

Garnet and clinopyroxene constitute the main minerals of the prograde associations in all skarn deposits, being excellent guides to determine the type of deposit, the physico-chemical conditions of the system and the initial composition of the fluids (Einaudi et al., 1981; Newberry, 1983; Meinert et al., 2005). The composition of garnet (Table 1, 2, 3, 4) and clinopyroxene (Table 5, 6) associated to scheelite mineralization and scheelite-free reaction skarn were plotted in the traditional triangular diagrams where the representative fields of worldwide mineralized skarns are shaded (Meinert, 1992; figure 8). All garnet and pyroxene analyses plot within the field of W skarn deposits, as expected.

5.1.1. CLASSIFICATION OF W SKARNS BASED ON GARNET CHEMISTRY

Tungsten skarns can be classified into strongly reduced (e.g., MacTung, CanTung, Dick and Hodgson, 1982), moderately reduced (e.g., Pine Creek, EEUU, Newberry, 1982) and oxidized (e.g., King Island, Australia, Kwak, 1978; Shizhuyuan, China, Lu et al., 2003), according to redox formation conditions (Newberry, 1983). Based on global W deposits, this distinction is based on the local geological setting, dominance of subcalcium member in garnet, Fe^{+2}/Fe^{+3} ratio, composition of the host rock (calcareous *vs* hematitic), abundance of clinopyroxene and its composition, and the enrichment in metals such as Mo, Sn and Cu. The relationship between subcalcic garnets and those of the *grandite* series (grossular-andradite), provides information about the reduced or oxidized nature of skarns, especially in those skarn deposits that have high contents of subcalcic garnets, such as scheelite skarns (Newberry, 1983). This author presented a study of garnets from the W skarn deposits of the West Coast of the United States and shows the proportional relationships between Alm-Sps and Ad-Gr, inferring the strongly reduced, moderately reduced or oxidized conditions of the skarns. According to Newberry (1983), moderately reduced tungsten skarns are characterized by a high Sps/Alm and Ad/Alm ratio, whereas the strongly reduced ones are characterized by a low Ad/Gr and Sps/Alm ratio. The relationship is directly proportional to the content of andradite. This is because the presence of high ionic radius cations at the *Y* structural sites (i.e., Fe^{+3} to Al^{+3}) results in the instability of small cations at the *X* structural sites (e.g., Fe^{+2}). In this way, the content of Mn^{+2} to stabilize Fe^{+2} must be greater in the andraditic garnets and therefore the proportional relationship between Ad/Gr and Sps/Alm is direct (Novak and Gibbs, 1971). Thus, at moderately reduced conditions, a high Sps/Alm ratio is required as the Ad/Grs ratio increases, whereas at strongly reduced conditions the andradite content that can be accommodated in the garnet is limited. The Ad/Gr molar ratio in Los Guindos garnets varies between ~ 0.02 - 0.30 for the zone I, 0.19 - 0.37 for the zone II, and 0.08 - 0.33 for the zone III. The Sps/Alm ratio is greater than 2:1 for garnet in all areas but the Ad/Grs is too low (< 0.5). According to the composition of garnet from early prograde zones, Los Guindos scheelite skarn can be classified as strongly reduced skarn of late-distal origin in all its prograde stages (Fig. 10). As can be deduced, the field of reduced W skarns is located along the side of the compositional triangle poor in the andraditic member due to Fe^{+3} deficiencies in the system and rich in subcalcium members (Mn^{+2}, Fe^{+2}).

5.1.2. COMPARISION WITH WORLDWIDE SKARN DEPOSITS

The most distinctive features of reduced W skarn deposits are high clinopyroxene/garnet ratios, subcalcic dominance on garnet composition due to low fO_2, Mo-poor or absent in scheelite and absence of magnetite, great depth of formation and reduced plutons involved in its origin (i.e., ilmenite-type granitoids; Newberry and Einaudi, 1981; Newberry, 1983; Newberry and Swanson, 1986; Kwak, 1987). The physical-chemical conditions of the main prograde and retrograde skarns and mineralization stage were developed under reduced W/R interaction settings. The occurrence of beryl instead of helvite in the prograde skarn of some mines could be due to the activity of Al-rich fluids that inhibited helvine formation following garnet crystallization in the initial prograde skarn evolution (Barton and Young, 2002); this was noted by Gordillo and Gay (1979) for the helvite formation in the Chingolo mine. The presence of Al-rich fluids is also registered in retrograde skarn as muscovite (sericite) and illite. The Al enrichment in skarn formation fluids is quite common in W-Sn skarns and has been observed in several worldwide W skarn deposits as in Lost River (Dobson, 1982), Shizhuyuan (Lu et al., 2003) and Lermontovskoe (Soloviev et al., 2017), related to highly differentiated granites in extensional (post-collisional and within plate) tectonic settings.

In W skarns is also common the presence of metamorphic aureoles of calc-silicate hornfels or reaction skarns enclosed by late ore skarn formation (Einaudi et al., 1981; Newberry 1982; Kwak, 1978, 1987; Lu et al., 2003). These reaction skarns are interpreted as the product of transition from early-distal metamorphism during magma crystallization through country rocks, to later-proximal metasomatism resulting in a coarse grained scheelite skarn. Baldo (1992) and Baldo and Verdecchia (2014) reported hornfels as contact metamorphic evidence of the Achalian batholith emplacement to the west of Los Guindos, over the N-S Carnerío river's course. However, no evidence of this contact aureole around the scheelite skarn bodies was found. At Los Guindos, the scheelite-free reaction skarn is reduced, supported by the Fe-rich composition of clinopyroxene, the high content of subcalcic molar proportions in garnets and the presence of sulfides such as pyrrhotite. Due to the depth of formation, it is common in most of the W skarn environments to find calc-silicate hornfels and reaction skarns formed from diffusional fluids in mixed carbonate-pelite sequences. These rocks commonly preceded skarn forming fluids (Einaudi et al., 1981; Kwak, 1987; Meinert et al., 2005). The calculated pressure of formation of 2.5 kbar for the scheelite-free reaction skarn is coincident with the range of 1.5 – 3 kbar obtained by apatite fission-track analyses and by metamorphic assemblages for the emplacement of the main phase of the Achala Batholith (Patiño and Patiño Douce, 1987; Jordan et al., 1989; Baldo, 1992). Field and textural evidence support that scheelite-free reaction skarn formed earlier than mineralized skarns, therefore the later should have formed at pressures not higher than 2.5 kb and probably much lower.

5.1.3. ACHALA GRANITIC MAGMATISM AND ITS RELATION WITH SKARN FERTILITY

Worldwide, reduced W skarn deposits are associated to calc-alkaline ilmenite-type granitoids with high degree of differentiation and crustal contamination, and associated with other incompatible elements (e.g., Sn, Mo, U, Nb, Ta; Newberry and Swanson, 1986). These evidences, together with correlation of major element chemistry of the Achala Batholith with granite-related skarn deposits worldwide (Fig. 12), allow assigning the formation of Los Guindos scheelite skarn to the Achalian magmatism. Also, some geochemical indicator ratios such as K/Rb vs SiO_2 and oxidized-reduced parameters (i.e., Blevin, 2004) applied to different Achala granite facies revealed highly compatible physical-chemical conditions of magma with the formation of fertile skarns (e.g., highly evolved and moderately oxidized conditions, figure 13). The potential of granite magmas on skarn fertility based on several physico-chemical parameters has been noted in different skarn deposits worldwide (e.g., Zhong et al., 2018, 2021). In addition, the high content of F in Los Guindos skarn, represented not only as late fluorite, but also in fluorine enriched minerals such as F-rich actinolite, F-bearing garnet, fluorapatite and vesuvianite are consistent with the involvement of metasomatic fluids derived from this F-rich magmatism (Lira, 1987; Galindo et al., 1996; Lira et al., 1996; Dorais et al., 1997; Franchini et al., 1998a, 1988b; Franchini and Lira, 1999; Coniglio et al., 2000; Sureda et al., 2006).

5.1.4. LOS GUINDOS SCHEELITE SKARN U-Pb AGE

The U-Pb age of prograde garnet of the scheelite skarn in LGMG is 361 ± 11 Ma. The first age for the Achala Batholith using conventional U-Pb in zircon was published by Dorais et al. (1997) for the porphyritic to equigranular dominant facies of the granitic complex obtaining an age of 368 ± 2 Ma and of 367.4 ± 5 Ma in cumulate apatite-biotite rich enclaves within the same facies. Subsequently, Rapela et al. (2008) dated U-Pb SHRIMP in zircons obtaining ages of 379 ± 4 Ma and 369 ± 3 Ma, concordant with those obtained by Dorais et al. (1997). Dahlquist et al. (2013a, 2013b) obtained by LA-ICP-MS an average age of 369 Ma and 370 ± 8 Ma for granodioritic/monzogranitic and porphyritic monzogranite facies. The hybrid-NYF intragranitic pegmatites of the batholith were originally dated by Linares and Latorre (1969) and Linares and Kleiner (1973) by K/Ar in muscovite and biotite, obtaining cooling ages between 356 ± 10, 350 ± 30 and 352 ± 25 Ma. Accordingly, Galliski et al. (2021) got a concordia LA-ICP-MS $^{238}U/^{206}Pb$ age of 354.8 ± 1.68 Ma for a columbite group mineral of the intermediate zone of the Gigante intragranitic pegmatite in the Achala batholith, which confirms the extension of the Achala magmatism into the Lower Carboniferous. Nevertheless, we interpret that the garnet age represents the age of metasomatic-hydrothermal fluids exsolved from some underlying buried evolved granite pluton, facies or pegmatite swarm that belongs to the Late Devonian-Lower Carboniferous Achalian tectonomagmatic event.

6. CONCLUSION

Los Guindos scheelite skarn deposit is a strongly reduced W skarn based on its prograde and retrograde mineral chemistry. Garnet and clinopyroxene compositions are predominantely Mn-Fe rich in prograde skarn where a compositional variation is observed from core to rim in individual crystals and from proximal to distal prograde zones, which can be attributed to the evolution of water/rock interaction during skarn formation. Scheelite mineralization could have been triggered by fluid-rock replacements during the retrograde skarn process due to Ca^{+2} release into the fluid and reached its deposition peak during a following hydrothermal infilling stage. The evolutive transition between these two stages was gradual and developed in space and temporal progression. This scheelite skarn shares similarities with other W-Sn reduced skarn deposits worldwide, like the presence of incompatible elements associated with W such as Bi-Sn-Ag, subcalcic garnet, Mo-free scheelite, absence of magnetite, reaction skarn formation prior to ore skarn, mineral indicators of late Al-rich fluids, within plate tectonic setting, among others. The U-Pb age in garnet of the scheelite skarn in LGMG is 361 ± 11 Ma; it is consistent with the age range between 383-366 Ma given to the main granites of the Achala Batholith and somehow older than the cooling ages of intragranitic pegmatites. For this reason, and together with geochemical and evolution parameters of the main Achala Batholith crystallization and fractionation, the origin of the skarn forming fluids can be attributed to the calc-alkaline, ilmenite-bearing A-type peraluminous Achala magmatism of Devonian age. The Los Guindos scheelite skarn should be considered as part of the dawning stage of the Devonian Metallogenic Epoch (Skirrow et al., 2000; Franchini et al., 2005). However, its U-Pb age error encompasses the Devonian-Carboniferous (D/C) boundary time span; a reason that allows to consider the Los Guindos scheelite skarn formation within the Devonian-Carboniferous Metallogenic Epoch.

7. ACKNOWLEDGEMENTS

This study was supported by programs of the Chinese Academy of Sciences (132744KYSB20190039, GJHZ1776) and by the Secretaría de Ciencia y Tecnología de la Universidad Nacional de Córdoba, Argentina (Res. SeCyT-UNC N° 411/18 and N° 99/19). María J. Espeche and R. Lira are grateful for the assistance of Dr. Alina B. Guereschi with microprobe analyses. The authors deeply appreciate the enriching observations made by two anonymous reviewers and by Dr. Nora Rubinstein as Associate Editor of Ore Geology Reviews.

8. REFERENCES

Agulleiro Insúa, L., Coniglio, J.E., D'Eramo, F.J., Pinotti, L.P., Demartis, M., Petrelli, H., 2013. Plutón Capilla del Monte, Sierras de Córdoba: Nuevos aportes metalogenéticos, cartográficos y petrológicos. XI MINMET, San Juan. 275-280.

Ametrano, S., 1999. El distrito scheelítico de la sierra de Altautina, Córdoba, in: Zappettini, E.O. (Ed), Recursos Minerales de la República Argentina, Instituto de Geología y Recursos Minerales SEGEMAR, Anales 35, Buenos Aires, pp. 233-239.

Angelelli, V., 1984. Yacimientos Metalíferos de la República Argentina, Comisión de Investigaciones Científicas de la Provincia de Buenos Aires, Buenos Aires.

Astini, R., Del Papa, C., 2014. Cubierta sedimentaria paleozoica superior, in: Martino, R.D., Guereschi, A.B. (Eds.), Geología y recursos naturales de la provincia de Córdoba, Relatorio del XIX Congreso Geológico Argentino, Asociación Geológica Argentina, Córdoba, pp. 393-420.

Astini, R., Oviedo, N., 2014. Cubierta sedimentaria mesozoica, in: Martino, R.D., Guereschi, A.B. (Eds.), Geología y recursos naturales de la provincia de Córdoba, Relatorio del XIX Congreso Geológico Argentino, Asociación Geológica Argentina, Córdoba, pp. 435-372.

Astini, R.A., Tauber, A.A., Marengo, H.G., Oviedo, N., 2014. Cubierta cenozoica (Paleógeno-Neógeno), in: Martino, R.D., Guereschi, A.B. (Eds.), Geología y recursos naturales de la provincia de Córdoba, Relatorio del XIX Congreso Geológico Argentino, Asociación Geológica Argentina, Córdoba, pp. 539-589.

Baldo, E.G., 1992. Estudio petrológico y geoquímico de las rocas ígneas y metamórficas entre Pampa de Olaen y Characato, extremo norte de la Sierra Grande de Córdoba. República Argentina. PhD Thesis, National University of Córdoba, Córdoba.

Baldo, E.G., Verdecchia, S.O., 2014. Las metamorfitas de contacto asociadas al magmatismo achaliano de las Sierras de Córdoba, in: Martino, R.D., Guereschi, A.B. (Eds.), Geología y recursos naturales de la provincia de Córdoba, Relatorio del XIX Congreso Geológico Argentino, Asociación Geológica Argentina, Córdoba, pp. 349-363.

Baldo, E.G., Rapela, C.W., Pankhurst, R.J., Galindo, C., Casquet, C., Verdecchia, S.O., Murra, J.A., 2014. Geocronología de las Sierras de Córdoba: revisión y comentarios, in: Martino, R.D., Guereschi, A.B. (Eds.), Geología y recursos naturales de la provincia de Córdoba, Relatorio del XIX Congreso Geológico Argentino, Asociación Geológica Argentina, Córdoba, pp. 845–864.

Barton, Md., Young, S., 2002. Non-pegmatitic Deposits of Beryllium: Mineralogy, Geology, Phase Equilibria and Origin, in: Grew, E.S. (Ed.), Beryllium-Mineralogy, Petrology, and Geochemistry. Reviews in Mineralogy and Geochemistry. 50 (1), 591-691.

Biglia, M.E., Lira, R., Sfragulla, J.A., 2016. Nuevos datos mineralógicos, petrográficos y metalogenéticos del distrito minero Agua de Ramón, departamento Minas, Córdoba. Revista de la Asociación Geológica Argentina. 73 (2), 225-241.

Blasón, R., Bello, C., Álvarez, J., Zarco, J., 2014. Recursos uraníferos, in: Martino, R.D., Guereschi, A.B. (Eds.), Geología y recursos naturales de la provincia de Córdoba, Relatorio del XIX Congreso Geológico Argentino, Asociación Geológica Argentina, Córdoba, pp. 1189–1205.

Blevin, P.L., 2004. Redox and Compositional Parameters for Interpreting the Granitoid Metallogeny of Eastern Australia: Implications for Gold-rich Ore Systems. Resource Geology. 54 (39), 241–252.

Bonalumi, A.A., Sfragulla, J.A., Jerez, D.G., 1999a. Fluorita de las Sierras Pampeanas de Córdoba, in: Zappettini, E.O. (Ed), Recursos Minerales de la República Argentina, Instituto de Geología y Recursos Minerales SEGEMAR, Anales 35, Buenos Aires, pp. 1015–1020.

Bonalumi, A.A., Martino, R.D., Baldo, E.G., Zarco, J., Sfragulla, J., Carignano, C.A., Kraemer, P., Escayola, M., Tauber, A., Cabanillas, A., Juri, E., Torres, B., 1999b. Hoja Geológica 3166-IV, Villa Dolores. Provincias de Córdoba, La Rioja y San Luis, Instituto de Geología y Recursos Minerales, Servicio Geológico Minero Argentino, Buenos Aires.

Brodtkorb de, M.K., Brodtkorb, A., 1999. Yacimientos de scheelita asociados a anfibolitas y rocas calcosilicáticas, San Luis, in: Zappettini, E.O. (Ed), Recursos Minerales de la República Argentina, Instituto de Geología y Recursos Minerales SEGEMAR, Anales 35, Buenos Aires, pp. 257-269.

Brodtkorb de, M.K., Fernández, R., Pezzutti, N., 1999. Yacimientos de wolframio asociados a metavulcanitas y metasedimentitas de San Luis, in: Zappettini, E.O. (Ed), Recursos Minerales de la República Argentina, Instituto de Geología y Recursos Minerales SEGEMAR, Anales 35, Buenos Aires, pp. 323-335.

Brodtkorb, M.K de, Coniglio, J., Miró, R., 2014. Yacimientos metalíferos y metalogenia, in: Martino, R.D., Guereschi, A.B. (Eds.), Geología y recursos naturales de la provincia de Córdoba, Relatorio del XIX Congreso Geológico Argentino, Asociación Geológica Argentina, Córdoba, pp. 1025-1075.

Candiani, J.C., Zarco, J., Gamba, M.T., Jerez, D., 2007. Hoja Geológica 3166-24: Pampa de Olaen. Boletín 234-bis. Programa Nacional de Cartas Geológicas de la República Argentina 1:100.000. SEGEMAR, Instituto de Geología y Recursos Minerales, Buenos Aires.

Carignano, C.A., Kröhling, D., Degiovanni, S., Cioccale, M.A., 2014. Geomorfología, in: Martino, R.D., Guereschi, A.B. (Eds.), Geología y recursos naturales de la provincia de Córdoba, Relatorio del XIX Congreso Geológico Argentino, Asociación Geológica Argentina, Córdoba, pp. 747-821.

Coniglio, J., Xavier, R.P., Pinotti, L., D'Eramo, F., 2000. Ore forming fluid of vein-type fluorite deposits of Cerro Áspero batholith, southern Córdoba Province, Argentina. International Geology Review. 42 (4), 368–383.

Coniglio, J., Perez Xavier, R., Pinotti, L., D`Eramo, F., Petrelli, H., Ducart, D., 2001. Evolución de fluidos hidrotermales y la formación de vetas de cuarzo-wolframita del

Distrito Minero Cerro Áspero, Córdoba. 7º Congreso Argentino de Geología Económica, Salta. 1, 87– 93.

Cuervo, S., 1988. Análisis multivariado de algunas manifestaciones talcosas de la Sierra de Córdoba. Underdegree thesis, National University of Córdoba, Córdoba.

D'Eramo, F.J., Pinotti, L.P., Bonalumi, A.A., Sfragulla, J., Demartis, M., Coniglio, J., Baldo, E.G., 2014. El magmatismo ordovícico en las Serras Pampeanas de Córdoba, in: Martino, R.D., Guereschi, A.B. (Eds.), Geología y recursos naturales de la provincia de Córdoba, Relatorio del XIX Congreso Geológico Argentino, Asociación Geológica Argentina, Córdoba, pp. 233-254.

Dahlquist, J.A., Alasino, P.H., Bello, C., 2013a. Devonian F-rich peraluminous A-type magmatism in the proto-Andean foreland (Sierras Pampeanas, Argentina): geochemical constraints and petrogenesis from the western-central región of the Achala batholith. Mineralogy and Petrology. DOI 10.1007/s00710-013-0308-0.

Dahlquist, J.A., Pankhurst, R.J., Gaschnig, R.M., Rapela, C.W., Casquet, C., Alasino, P.H., Galindo, C., Baldo, E.G., 2013b. Hf and Nd isotopes in Early Ordovician to Early Carboniferous granites as monitors of crustal growth in the Proto-Andean margin of Gondwana. Gondwana Research. 23, 1617–1630.

Demange, M., Baldo, E.G., Martino, R.D., 1993. Structural evolution of the Sierras de Córdoba (Argentina). Second ISAG, Oxford (UK), 513-516.

Demange, M., Álvarez, J.O., López, L., Zarco, J.J., 1996. The Achala Batholith (Córdoba, Argentina): a composite intrusion made of five independent magmatic suites. Magmatic evolution and deuteric alteration. Journal of South American Earth Sciences. 9 (1-2), 11–25.

Dick, L.A., Hodgson, C.J., 1982. The MacTung W-Cu(Zn) contact metasomatic and related deposits of the Northeastern Canadian Cordillera. Economic Geology. 77, 845-867.

Dobson, D.C., 1982. Geology and alteration of the Lost River Tin-Tungsten-Fluorine Deposit, Alaska. Economic Geology. 77, 1033-1052.

Dorais, M.J., Lira, R., Chen, Y., Tingey, D., 1997. Origin of biotite-apatite-rich enclaves, Achala batholith, Argentina. Contributions to Mineralogy and Petrology. 130, 31-46.

Einaudi, M.T., Meinert, L.D. and Newberry, R.J. 1981. Skarn deposits. Economic Geology. 75, 317-391.

Enriquez, E., Iocco, M., Ramos, G., Morosini, A., 2019. Mineralización de scheelita en ortoanfibolitas, mina El Colatillo, provincia de San Luis, Argentina. XIII MINMET – IV PIMMA, Córdoba. 301-302.

Espeche, M.J., Lira, R., 2018. A review of scheelite-bearing skarns in the Eastern Pampean Ranges: mining records and mineralogical data of Los Guindos mining group, Pampa de Olaen district, Córdoba, Argentina. 15th Quadrennial IAGOD International Association on the Genesis of Ore Deposits Symposium, Salta. 221-222.

Espeche, M.J., Lira, R., 2019a. El origen del wolframio en los depósitos de scheelita de las Sierras Pampeanas de Córdoba: ¿estratoligado o magmático?. XIII MINMET – IV PIMMA, Córdoba. 298-299.

Espeche, M.J., Lira, R., Gereschi, A.B., 2019b. Zincocromita en un skarn del grupo minero Los Guindos, Córdoba: primer registro en Argentina. XIII MINMET – IV PIMMA, Córdoba. 408-414.

Espeche, M.J., Lira, R., 2020. Pyrophanite in a scheelite skarn, Sierras Pampeanas, Córdoba, Argentina: a new paragenetic occurrence. XII Congreso Argentino de Geología Económica, La Plata. 80-86.

Etcheverry, R., Brodtkorb de, M.K., 1999. Yacimiento de wolframio vetiforme de San Luis, in: Zappettini, E.O. (Ed), Recursos Minerales de la República Argentina, Instituto de Geología y Recursos Minerales SEGEMAR, Anales 35, Buenos Aires, pp. 591-600.

Fernández Lima, J.C., Jurotan, A., Kroger, J., Aspilcueta, J., 1963. Informe preliminar de los grupos wolframíferos Cerro Áspero, Lambaré, Constancia y Fischer: Informe Técnico nº 18, Ministerio de Economía de la Nación, Secretaría de Industria y Minería, Buenos Aires.

Franchini, M., Lira, R., 1998. Granates con flúor en skarns de las Sierras Pampeanas de Córdoba, Argentina. 4º Reunión de Mineralogía y Metalogenia, Universidad Nacional del Sur, MINMET´98-EDIUNS, Bahía Blanca. 93–103.

Franchini, M., Lira, R., Sfragulla, J., 1998a. Zonación mineralógica y evolución de los fluidos en el skarn Copina, provincia de Córdoba (64°39' O - 31°30' S). Revista de la Asociación Geológica Argentina. 53 (2), 197–211.

Franchini, M., Lira, R., Sfragulla, J., 1998b. El skarn Cañada del Puerto (31°25' LS - 64° 54' LO), Provincia de Córdoba: otro ejemplo de metasomatismo caracterizado por fluidos ricos en agua, hidrógeno y flúor. Revista de la Asociación Geológica Argentina. 53 (2), 247–260.

Franchini, M., Lira, R., Meinert, L.D., Ríos, F.J., Poklepovic, M.F., Impiccini, A., Millone, H.A., 2005. Na-Fe-Ca Alteration and LREE (Th-Nb) Mineralization in Marble and Granitoids of Sierra de Sumampa, Santiago del Estero, Argentina. Economic Geology. 100, 733-764.

Galindo, C., Pankhurst, R.J., Casquet, C., Coniglio, J., Baldo, E., Rapela, C.W., Saavedra J., 1996. Age, Sr and Nd-Isotope Systematics and origin of two Fluorite Lodes, Sierras Pampeanas, Argentina. International Geology Review. 39, 948–954.

Galliski, M.A., 1993. La Provincia Pegmatítica Pampeana. I: Tipología y distribución de sus distritos económicos. Revista de la Asociación Geológica Argentina. 49 (1-2), 99–112.

Galliski, M.A., 1994. La Provincia Pegmatítica Pampeana. II. Metalogénesis de sus distritos económicos. Revista de la Asociación Geológica Argentina. 49 (1-2), 113–122.

Galliski, M.A., Sfragulla, J., 2014. Las pegmatitas graníticas de las Sierras de Córdoba, in: Martino, R.D., Guereschi, A.B. (Eds.), Geología y recursos naturales de la provincia de Córdoba, Relatorio del XIX Congreso Geológico Argentino, Asociación Geológica Argentina, Córdoba, pp. 365-388.

Galliski, M.A., Márquez Zavalía, M.F., Pagano, D.S., Škoda, R., 2019. The Totoral tungsten district, San Luis, Argentina: W-(Au, Sb) bearing sills associated to late-collisional S-type leucogranites. XIII MINMET – IV PIMMA, Córdoba. 426-427.

Galliski, M.A., von Quadt, A., Márquez-Zavalía, M.F. 2021. LA-ICP-MS U-Pb columbite ages and trace-element signature from rare-element granitic pegmatites of the Pampean Pegmatite Province, Argentina. Lithos. https://doi.org/10.1016/j.lithos.2021.106001.

Gamba, M.T., 1996. Minerales de Ag, Bi y Sn en la mina Loma Pajosa, distrito minero scheelítico Los Guindos, Córdoba, Argentina. Reunión de Mineralogía y Metalogenia, No. 3, Publicación del INREMI, Universidad Nacional de La Plata. 119-121.

González Chiozza, S., 2021. Origin and Evolution of the W mineralization in the Intrusion-related Hydrothermal Deposits of the Cerro Áspero Mining District, Sierras Pampeanas, Argentina. Anuario do Instituto de Geociencias. 44, 1-16.

Gordillo, C.E., Lencinas, A.N., 1979. Sierras Pampeanas de Córdoba y San Luis. 2º Simposio de Geología Regional Argentina. Academia Nacional de Ciencias, Córdoba. 1, 577–650.

Grew, E.S., Locock, A.J., Mills, S.J., Galuskina, I.O., Galuskin, E.V., Hålenius, U., 2013. Nomenclature of garnet supergroup. American Mineralogist. 98, 785-811.

Guereschi, A.B., Martino, R.D., 2014. Las migmatitas de las Sierras de Córdoba, in: Martino, R.D., Guereschi, A.B. (Eds.), Geología y recursos naturales de la provincia de Córdoba, Relatorio del XIX Congreso Geológico Argentino, Asociación Geológica Argentina, Córdoba, pp. 67-94.

Herrmann, C.J., 2002. Estudio geológico del distrito wolframífero Ambul, Provincia de Córdoba. PhD Thesis, University of Buenos Aires, Buenos Aires.

Herrmann, C.J., Tourn, S.M., 2002. Metalogenia de vetas wolframíferas en el norte y oeste de las Sierras de Córdoba. Actas del 15° Congreso Geológico Argentino, El Calafate. 439-444.

Holmberg, E., 1960. Reseña geológica del distrito minero de Pampa de Olaen, Cosquín, provincia de Córdoba. Dirección Nacional de Geología y Minería, Córdoba.

Hutchinson, M.N., Scott, S.D., 1981. Sphalerite geobarometry in the Cu-Fe-Zn-S system. Economic Geology. 76, 143-153.

Jordan, T.E., Zeitler, P., Ramos, V., Gleadow, A.J.W., 1989. Thermochronometric data on the development of the basement peneplain in the Sierras Pampeanas, Argentina. Journal of South American Earth Sciences. 2 (3), 207–222.

Kay, S.M., Gordillo, C.E., 1994. Pocho volcanic rocks and the melting of depleted continental lithosphere above a shallowly dipping subduction zone in the central Andes. Contributions to Mineralogy and Petrology. 117, 25–44.

Kwak, T.A.P., 1978. The conditions of formation of the King Island scheelite contact skarn, King Island, Tasmania, Australia. American Journal of Science. 278, 969-999.

Kwak, T.A.P., 1987. W-Sn skarn deposits and related metamorphic skarn and granitoids. Developments in Economic Geology, 24. Elsevier, 415 p. Amsterdam.

Lapidus, A., Rossi, N., 1959. Las minas de tungsteno de Agua de Ramón, Departamento Minas, Provincia de Córdoba. Dirección Nacional de Geología y Minería, Buenos Aires.

Linares, E., Kleiner, L., 1973. Biotita SJ-1, patrón de laboratorio para el método potasio-argón. 5º Congreso Geológico Argentina, Córdoba. 395–403.

Linares, E., Latorre, C.O., 1969. Edades potasio-argón y plomo-alfa de rocas graníticas de las provincias de Córdoba y de San Luis. 4º Jornadas Geológicas Argentinas, Mendoza. 195–204.

Lira, R., 1987. Episienitas feldespáticas y su relación con depósitos uraníferos en el batolito de Achala, provincia de Córdoba. Revista de la Asociación Geológica Argentina. 42 (3-4), 388–406.

Lira, R., Gay, H.D., 1999. Clinozoisita rosada en las Sierras de Córdoba. Revista de la Asociación Geológica Argentina. 54(2), 109-122.

Lira, R., Kirschbaum, A.M., 1990. Geochemical evolution of granites from the Achala batholith of the Sierras Pampeanas, Argentina, in: Kay, S.M., Rapela, C.W. (Eds.), Plutonism from Antarctica to Alaska, Geological Society of America, Boulder, Colorado, pp. 67–76.

Lira, R., Ripley, E.M., Españón, A., 1996. Meteoric water induced selvage-style greisen alteration in the Achala Batholith, central Argentina. Chemical Geology. 133, 261–277.

Lira, R., Sfragulla, J., 2014. El magmatismo devónico-carbonífero: el batolito de Achala y plutones menores al norte del cerro Champaquí, in: Martino, R.D., Guereschi, A.B. (Eds.), Geología y recursos naturales de la provincia de Córdoba, Relatorio del XIX Congreso Geológico Argentino, Asociación Geológica Argentina, Córdoba, pp. 293-347.

Llambías, E., 1963. Estudio petrográfico de muestras de la zona de Pampa de Olaen, Córdoba. Dirección Nacional de Geología y Minería, Córdoba.

Lu, H.Z., Liu, Y., Youzhi Xu, C.W., Li, H., 2003. Mineralization and Fluid Inclusion Study of the Shizhuyuan W-Sn-Bi-Mo-F Skarn Deposit, Hunan Province, China. Economic Geology. 98, 955-974.

Lucero, H.N., 1956. Estudio geológico minero de las minas Mogotes de la Picaza, El Nahuel, Los Rodeítos y Cubierta, del Dto. Minero Pampa de Olaen, provincia de Córdoba. Dirección Nacional de Geología y Minería, Córdoba.

Ludwig, A.K.R., 1998. On the Treatment of Concordant Uranium-Lead Ages. Geochimica et Cosmochimica Acta. 62 (4), 665-676.

Martino, R.D., Guereschi, A.B., 2014. La estructura Neoproterozoica-Paleozoica inferior del complejo metamórfico de las Sierras de Córdoba, in: Martino, R.D., Guereschi, A.B. (Eds.), Geología y recursos naturales de la provincia de Córdoba, Relatorio del XIX Congreso Geológico Argentino, Asociación Geológica Argentina, Córdoba, pp. 95 – 128.

Massabie, A.C., 1982. Geología de los alrededores de Capilla del Monte y San Marcos, provincia de Córdoba. Revista de la Asociación Geológica Argentina. 37 (2), 153-173.

Meinert, L.D., 1992. Skarns and Skarn Deposits. Ore Deposits Models. Geoscience Canadá Reprint Series. 6 (2), 117-134.

Meinert, L.D., Dipple, G.M., Nicolescu, S., 2005. World Skarn Deposits. Economic Geology. 100th Anniversary Volume, 299-336.

Monsberger, G., 1990. Estudio geológico y petrológico del granito de la Mesa de la Mula Muerta y su entonno encajonante. Pampa de Olaen, Dpto. Punilla, Córdoba. Undergraduate thesis, National University of Córdoba, Córdoba.

Montenegro, T., Etcheverry, R.O., Leal, P.R., de Brodtkorb, M.K., 2009. Depósitos de scheelita asociados a lamprófiros/biotititas departamento San Martín, San Luis. Revista de la Asociación Geológica Argentina. 64 (3), 447 – 457.

Morales Cámera, M.M., Dahlquist, J.A., Garcia-Arias, M., Moreno, J.A., Galindo, C., Basei, M.A.S., Molina, J.F., 2020. Petrogenesis of the F-rich peraluminous A-type granites: An example from the devonian achala batholith (Characato Suite), Sierras Pampeanas, Argentina. Lithos. 378-379, 105792. https://doi.org/10.1016/j.lithos.2020.105792

Morimoto, N., Fabries, J., Ferguson, A.K., Ginzburg, I.V., Ross, M., Seifert, F.A., Zussman, J., Aoki, K., Gottardi, G., 1988. Nomenclature of pyroxenes. American Mineralogist. 73, 1123-1133.

Mutti, D., González Chiozza, S., 2005. Evolución petrotectónica del distrito minero Cerro Áspero y modelo de emplazamiento de los depósitos wolframíferos, Córdoba. Revista Asociación Geológica Argentina. 60 (1), 159–173.

Newberry, R.J., Einaudi, M.T., 1981. Tectonic and geochemical setting of tungsten skarn mineralization in the Cordillera. Arizona Geological Society Digest .14, 99–111.

Newberry, R.J., 1983. The formation of subcalcic garnet in scheelite-bearing skarns. Canadian Mineralogist. 21, 529 – 544.

Newberry, J.R., Swanson, S.E., 1986. Scheelite skarn granitoids: an evaluation of the roles of magmatic source and process. Ore Geology Reviews. 1, 57-81.

Novak, G.A., Gibbs, G.V., 1971. The crystal chemistry of the silicate garnets. American Mineralogist. 56, 791-825.

Oliveri, J., 1954. Grupo minero de Olaen. Yacimientos de scheelita, dpto. Punilla, provincia de Córdoba. Dirección Nacional de Geología y Minería, Córdoba.

Oliveri, J., 1957. Grupo minero de Pampa de Olaen. Dirección Nacional de Geología y Minería, Córdoba.

Patiño, M.G., Patiño Douce, A.E., 1987. Petrología y petrogénesis del batolito de Achala, provincia de Córdoba, a la luz de la evidencia de campo. Revista de la Asociación Geológica Argentina. 42 (1-2), 201– 205.

Pezzutti, N., 1982. Informe petrográfico del Distrito Minero Los Guindos, Córdoba. Instituto Nacional de Geología y Minería, Buenos Aires.

Pinotti, L.D., Coniglio, J.E., D'Eramo, F.J., Demartis, M., Otamendi, J.E., Fagiano, M.R. and Zambroni, N.E. 2014. El magmatismo Devónico: Geología del batolito de Cerro Áspero. In Geología y recursos naturales de la provincia de Córdoba (Martino, R.D. and Guereschi, A.B. eds.). Relatorio del XIX Congreso Geológico Argentino: 255-276. Córdoba.

Rapela, C.W., 1982. Aspectos geoquímicos y petrológicos del batolito de Achala, provincia de Córdoba. Revista de la Asociación Geológica Argentina. 37 (3), 313–330.

Rapela, C.W., Baldo, E.G., Pankhurst, R.J., Fanning, C.M., 2008. The Devonian Achala Batholith of the Sierras Pampeanas: F-rich, aluminous A-type granites. 6º South American Symposium on Isotope Geology, Río Negro. 1-8.

Rimann, E., 1918. Estudio geológico de la Sierra Chica entre Ongamira y Dolores. Boletín de la Academia Nacional de Ciencias. 23, 129–202.

Seman, S., Stockli, D.F., McLean, N.M., 2017. U-Pb geochronology of grossular-andradite garnet. Chemical Geology. 460, 106–116.

Skirrow, R.G., 1997. Economic Geology of the Sierras Septentrionales of Córdoba 1:250000 map sheet, in: Lyons, P., Skirrow, R.G., Stuart-Smith, P.G. (Eds.), Report on geology and metallogeny of the Sierras Septentrionales de Córdoba 1:250.000 map sheet, Buenos Aires, pp. 68-115.

Skirrow, R.G., Camacho, A., Lyons, P., Pieters, P.E., Sims, J.P., Stuart-Smith, P.G., Miró, R.C. 2000. Metallogeny of the southern Sierras Pampeanas, Argentina: Geological, ^{40}Ar-^{39}Ar dating and stable isotope evidence for Devonian Au, Ag-Pb-Zn and W ore formation. Ore Geology Reviews. 17, 39-81.

Soloviev, S.G., Kryazhev, S.G., Dvurechenskaya, S.S., 2017. Geology, mineralization, and fluid inclusion characteristics of the Lermontovskoe reduced-type tungsten (±Cu, Au, Bi) skarn deposit, Sikhote-Alin, Russia. Ore Geology Reviews. 89, 15–39.

Sureda, R., Lira, R., Colombo, F., 2006. Gustavita, $PbAgBi_3S6$-$P2_1/c$, con los minerales de bismuto y plata en el 'skarn' Los Guindos, Pampa de Olaen, Córdoba, Argentina. Revista Geológica de Chile. 33 (1), 141-160.

Tourn, S., 1999. Los yacimientos de wolframio de Agua de Ramón, Córdoba, in: Zappettini, E.O. (Ed), Recursos Minerales de la República Argentina, Instituto de Geología y Recursos Minerales SEGEMAR, Anales 35, Buenos Aires, pp. 585-590.

Valdez, M.A., 1984. Cartografía geológica y estudio petromineralógico del distrito minero Los Guindos. Undergraduate thesis, National University of Córdoba, Córdoba.

Valley, J.W., Essene, E.J., Peacor, D.R., 1983. Fluorine-bearing garnets in Adirondack calc-silicates. American Mineralogist. 68, 444–448.

Vermeesch, P., 2018. IsoplotR: A free and open toolbox for geochronology. Geoscience Frontiers. 9, 1479-1493. doi:10.1016/j.gsf.2018.04.001

Whitney, D.L., Evans, B.W., 2010. Abbreviations for names of rock-forming minerals. American Mineralogist. 95, 185–187.

Yang, Y., Wu, F., Yang, J., Mitchell, R., Zhao, Z., Xie, L., Huang, C., Ma, Q., Yang, M., Zhao, H. 2018. U–Pb age determination of schorlomite garnet by laser ablation inductively coupled plasma mass spectrometry. Journal of Analytical Atomic Spectrometry. 33, 231–239.

Zang, Z., Dong, L., Lie, W., Zhao, H., Wang, X., Cai, K., Wan, B., 2019. Garnet U-Pb and O isotopic determinations reveal a shear-zone induced hydrothermal system. Scientific Reports. 9, 10382. doi:10.1038/s41598-019-46868-4

Zhong, S., Chengyou, F., Seltmann, R., Dolgopolova, A., Andersen J.C.Ø., Lia, D., Yud, M., 2018. Sources of fluids and metals and evolution models of skarn deposits in the Qimantagh metallogenic belt: A case study from the Weibao deposit, East Kunlun Mountains, northern Tibetan Plateau. Ore Geology Reviews. 93, 19-37.

Zhong, S., Li, S., Feng, C., Liu, Y., Santosh, M., He, S., Qu, H., Liu, G., Seltmann, R., Lai, Z., Wang, X., Song, Y., Zhou, J., 2021. Porphyry copper and skarn fertility of the northern Qinghai-Tibet Plateau collisional granitoids. Earth Sciences Review. 214, 103524.

Figure 1. Regional geologic map of the Oriental Pampean Ranges in Córdoba, San Luis and Santiago del Estero provinces of central Argentina, modified from Martino and Guereschi 2014a, with the location of the W skarn deposits.

Figure 2. a) Geological map of Los Guindos mining group with the location of the main scheelite mines (W), non confirmed mineralization outcrops (W?) and marble quarries that were declared as scheelite mines (M). 1: La Salamanca (W); 2: Chingolo (W); 3: Los Rodeítos (W); 4: Nahuel (W); 5: Mogote de la Picaza (W); 6: Loma Pajosa (W); 7: El Minerito (W); 8: Quebrada de los Contrabandistas (W); 9: La Confluencia (M); 10: Minero Don Zárate (M); 11: Los Caudillos (W); 12: Loma de la Paja (W); 13: Minero Don Cepeda (M); 14: Misteriosa Lámpara (W?); 15: Rundunes (W?); 16: Filón Colgado (W?); 17: Los Cuatreros (W?); 18: El Montonero (W); 19: Por Si Acaso (M); 20: Carnerillo 1 (M); 21: Los Fogones (W?); 22: El Mogote Alto (W?); 23: Quebrada Honda (W); 24: Cubierta (W); 25: Virgen del Valle N (W?); 26: Aguaitada N (W?); 27: Quebrada del Caliche (W?); 28: Virgen del Valle S (W?); 29: Los Reventones (W?); 30: Aguaitada S (W?); 31: Río Carnerillo (M); 32: Arroyo de los Guindos (M); 33: Los Guindos R (M); 34: Veta Pampa (W); 35:Escondida (M); 36: El Filón Grande (W?).

Figure 3. a) Reduced, scheelite-free reaction skarn overprinted by scheelite mineralized skarn (zone III), late infilling coarse-grained sphalerite (Sp2) and quartz veins. b) Schematic representation of “a”. Grt: garnet; Ves: vesuvianite.

Figure 4. a) Contact between zone I (Grt + Hlv) developed after replacement of an aplite-pegmatite dike, and zone II (Cpx + Grt) after marble replacement in El Minerito mine, the clear-cut contact is better shown in image “b”. c) Zone II (Cpx + Grt) scheelite-bearing (4 in the figure) is developed after calcic marble where it is common to find sphalerite filling

aggregates (3 in the figure) associated with scheelite (Sch), fluorite (Fl), calcite (Cal) and quartz (Qz). Some lenses of amphibolite (1 in the figure) are partially replaced by a barren amphibole-epidote-chlorite skarn (2 in the figure). d) Large vesuvianite (Ves) and garnet (Grt) crystals grown in voids in marble (zone III). The size of the crystals varies on each outcrop and represents a late association of zone II. e) and f) prismatic radial aggregates of acquamarine beryl (Brl) pseudomorphically replaced by an intergrown mixture of potassium feldspar and bertrandite. In image "e" the replacement is complete and is found in zone I while in "f" the replacement in partial and centripetal. g) Prismatic aggregates of plagioclase developed in a cavity open space found in an aplitic dike in the Loma Pajosa outcrop. These aggregates are also common in the Chingolo mine. h) Ordovician skarnified pegmatite showing an association of brown-orange garnet + clinopyroxene. i) Unmineralized masses of epidote + quartz representing distal/late fluids. j) Brown-red garnet skarn (± clinopyroxene) likely after amphibolite replacement, with masking Fe and Cu supergenic minerals in a gossan type environment. The scale in the photographs measures 9 cm.

Figure 5. a) Anisotropic euhedral garnet (Grt) crystal partially replaced by epidote. A relict of plagioclase (Pl) of the aplite-pegmatite dike replaced by sericite (Srct) is observed. b) Beryl crystal replaced by bertrandite and potassium feldspar (Brt + Kfs) and included by late quartz (Qz). Coarse-grained muscovite is present. c) Anisotropic garnet in contact with euhedral clinopyroxenes altered to actinolite-Potassium feldspar association, cut by intracrystalline fractures filled with calcite (Cal_3). This calcite is later than the infilling Cal_2 calcite. d) Aggregate of fibrous actinolite associated with epidote and potassium feldspar resulting from the total replacement of clinopyroxene, with final deposition of scheelite and fluorite. Note the linear trains of fluid inclusions in scheelite. e) Scheelite and polygranular clinopyroxene strongly replaced by actinolite included in late filling fluorite. Notice the late calcite veins (Cal_3) that cut scheelite and fluorite crystals. f) Euhedral vesuvianite crystals

with clinopyroxene inclusions included in filling epidote. g) Garnet crystals replaced at their edges by calcite (Cal_1) included in calcite (Cal_2) together with vesuvianite with clinopyroxene inclusions.

Figure 6. a) 3D Digital Elevation Model (DEM) of the Pampa de Olaen area and northeastern contact of the Achala Batholith with its most evolved leucogranite plutons (Characato, Mesa del Palmar and Mesa de la Mula Muerta). The associated long dashed lines represent interpreted fluid ascent channels. The short dashed lines show the probable underlying continuity to the east of the Achala granitic mass. Small outcrops of Achala granites are located 1.5 km west from the Los Guindos mining group (not represented in the DEM). The outlined rectangle is shown in b); b) Simplified scheme showing distribution of mineral assemblages in a representative scheelite-bearing skarn in Los Guindos mining group. Abbreviations after Whitney and Evans (2010), except for helvine: Hlv and fraipontite: Frp.

Figure 7. Paragenetic diagram showing the mineral sequence of Los Guindos Mining Group.

Figure 8. Ternary plots of garnet (a) and pyroxene (b) compositions for Los Guindos Mining Group following the world skarn deposits classification, adapted from Meinert et al. (2005). See text for explanation.

Figure 9. Compositional profile variation of zoned garnets from the three main prograde zones (A, B and C, i.e., zones I, II and III, respectively) of Los Guindos scheelite skarn, plotted on outlined schemes.

Figure 10. Garnet composition from Los Guindos Mining Group, expressed in terms of mole % grossular, andradite and almandine + spessartine (*pyralspite*), and comparison with W

skarn deposits worldwide after Newberry (1983). Data from strongly and moderately reduced skarn deposits are from Newberry (1983).

Figure 11. a) LA-ICP-MS U-Pb results of garnet with concordia and b) weighed mean average age. c) Pentagonal dodecahedron crystals of spessartine-grossular analyzed by U-Pb from the Chingolo mine; the sample belongs to the garnet + helvine zone. Calcite (Cal) and fluorite (not observed) are dominant cavity filling phases.

Figure 12. Correlation between major element whole rock chemistry of Achalian plutonic rocks and its association with the main skarn type deposits (after Meinert et al., 2005). The location of analyses of the Achala batholith granites above the W-skarn reference in d) could be explained due to strong late- to post-magmatic muscovitization of the Achalian granitoids, a widespread process that has affected most of the granite suites and facies of the batholith.

Figure 13. K/Rb versus SiO_2 and Redox classification scheme for different facies of Achala showing its highly evolved and moderately oxidized-reduced features, modified after Blevin (2004). Notice its affinity to form Sn±W and W-Mo-Bi deposits. FeO* refers to all Fe in the sample reported as FeO. VSO – very strongly oxidized, SO – strongly oxidized, MO – moderately oxidized, MR – moderately reduced, SR – strongly reduced.

1010 Figure 1 (Espeche et al.)

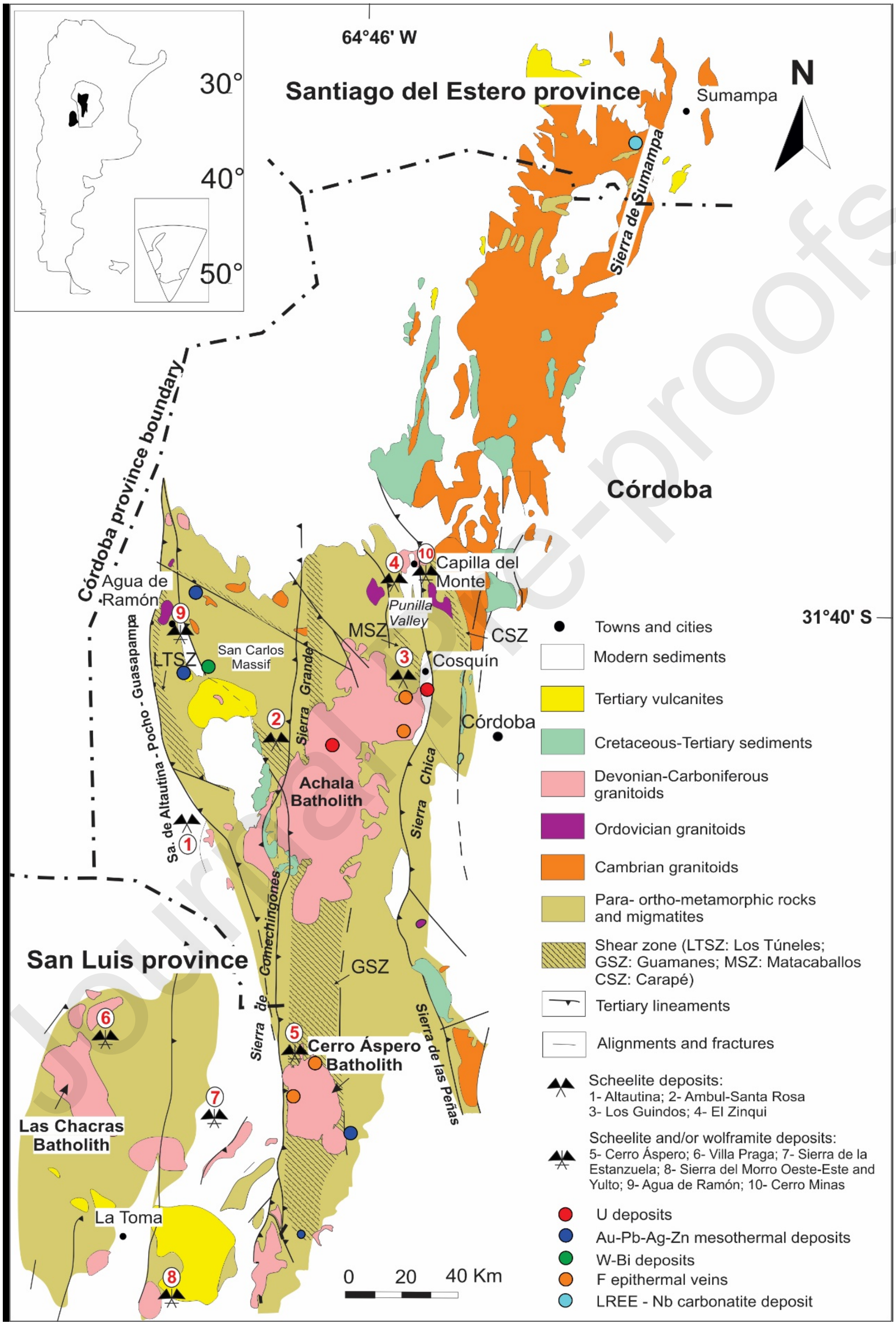

1011

Figure 2 (Espeche et al.)

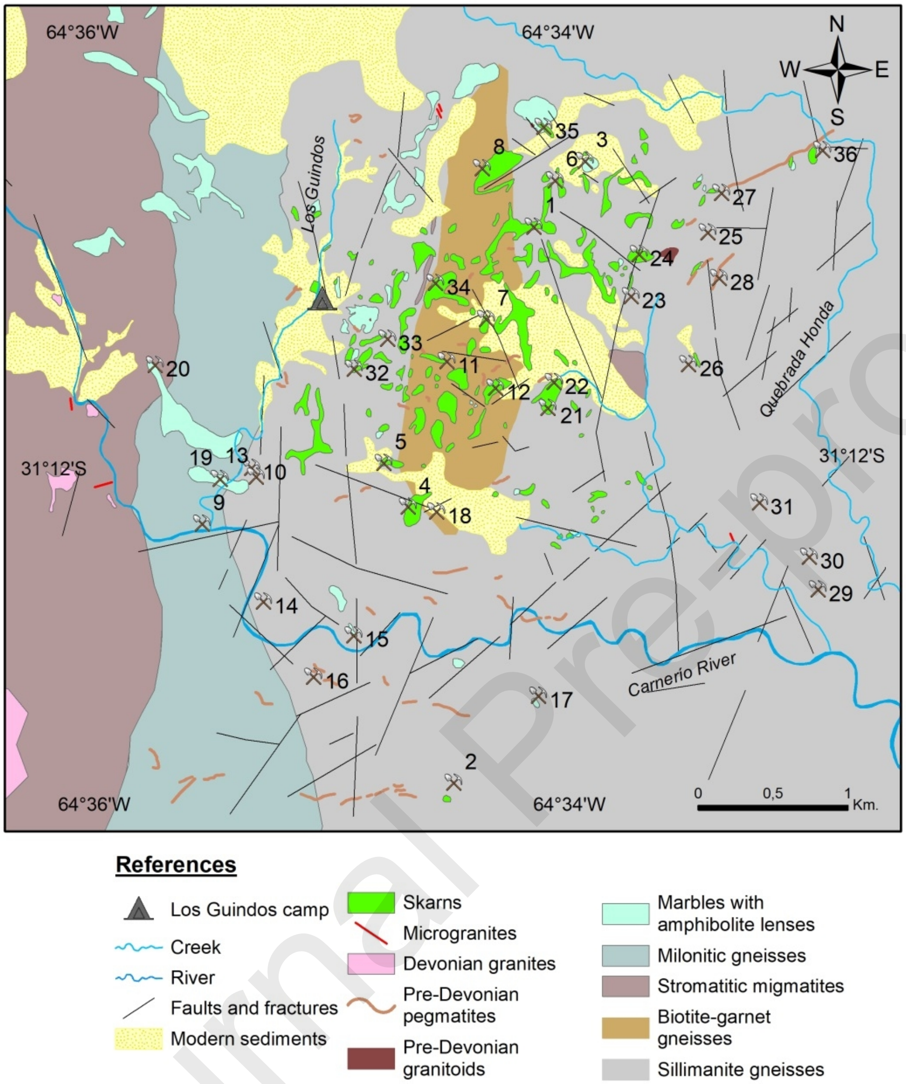

Figure 3 (Espeche et al.)

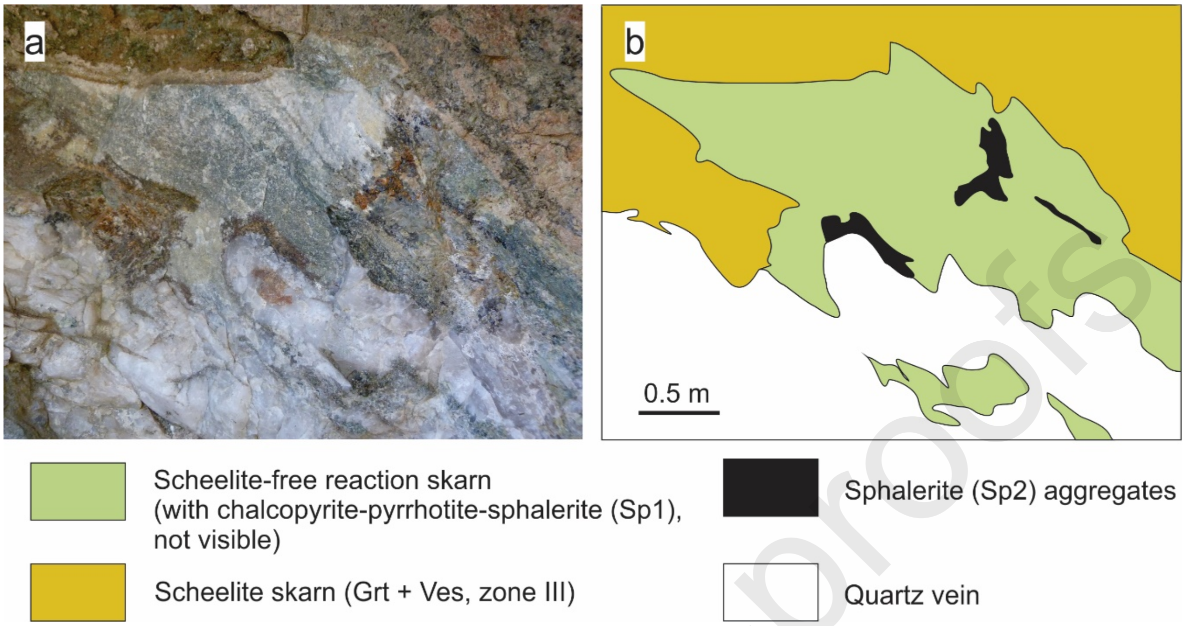

1039 Figure 4 (Espeche et al.)

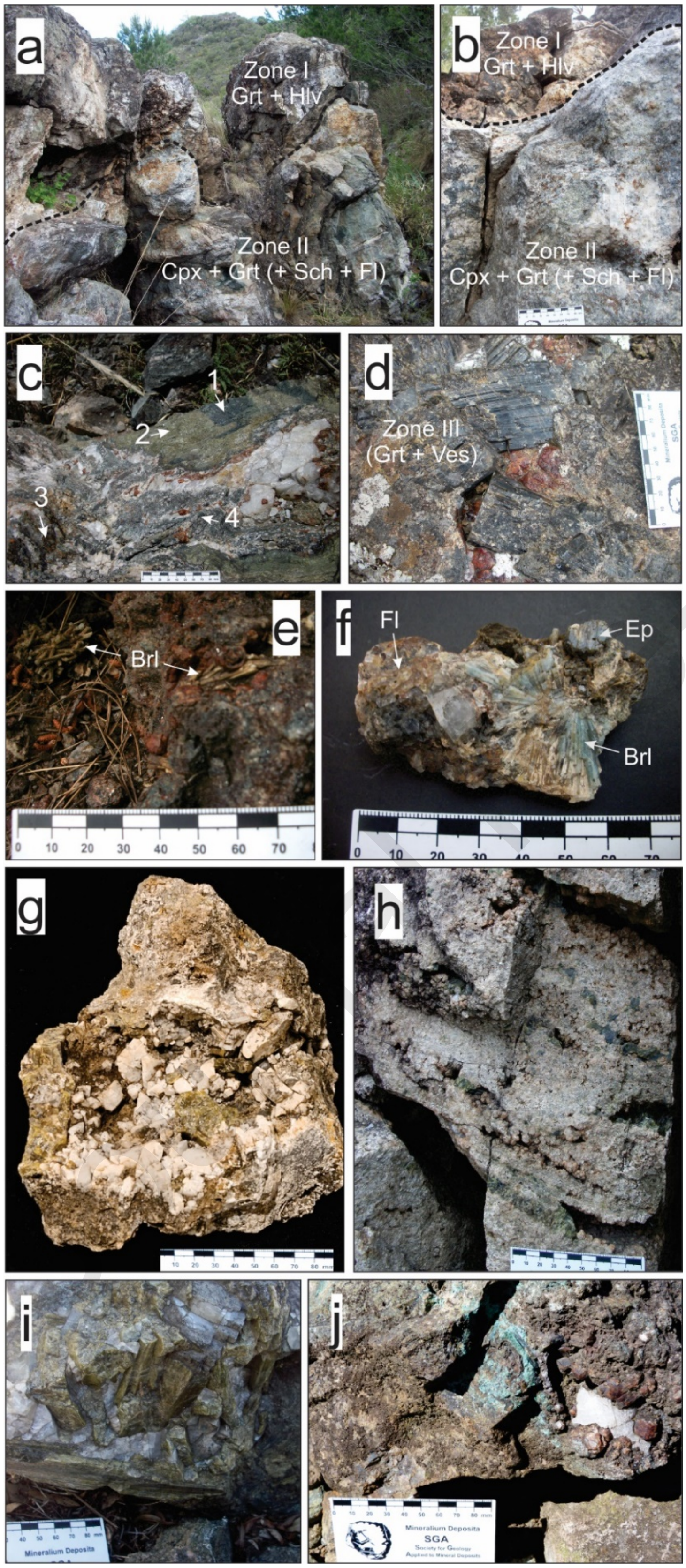

1040

Figure 5

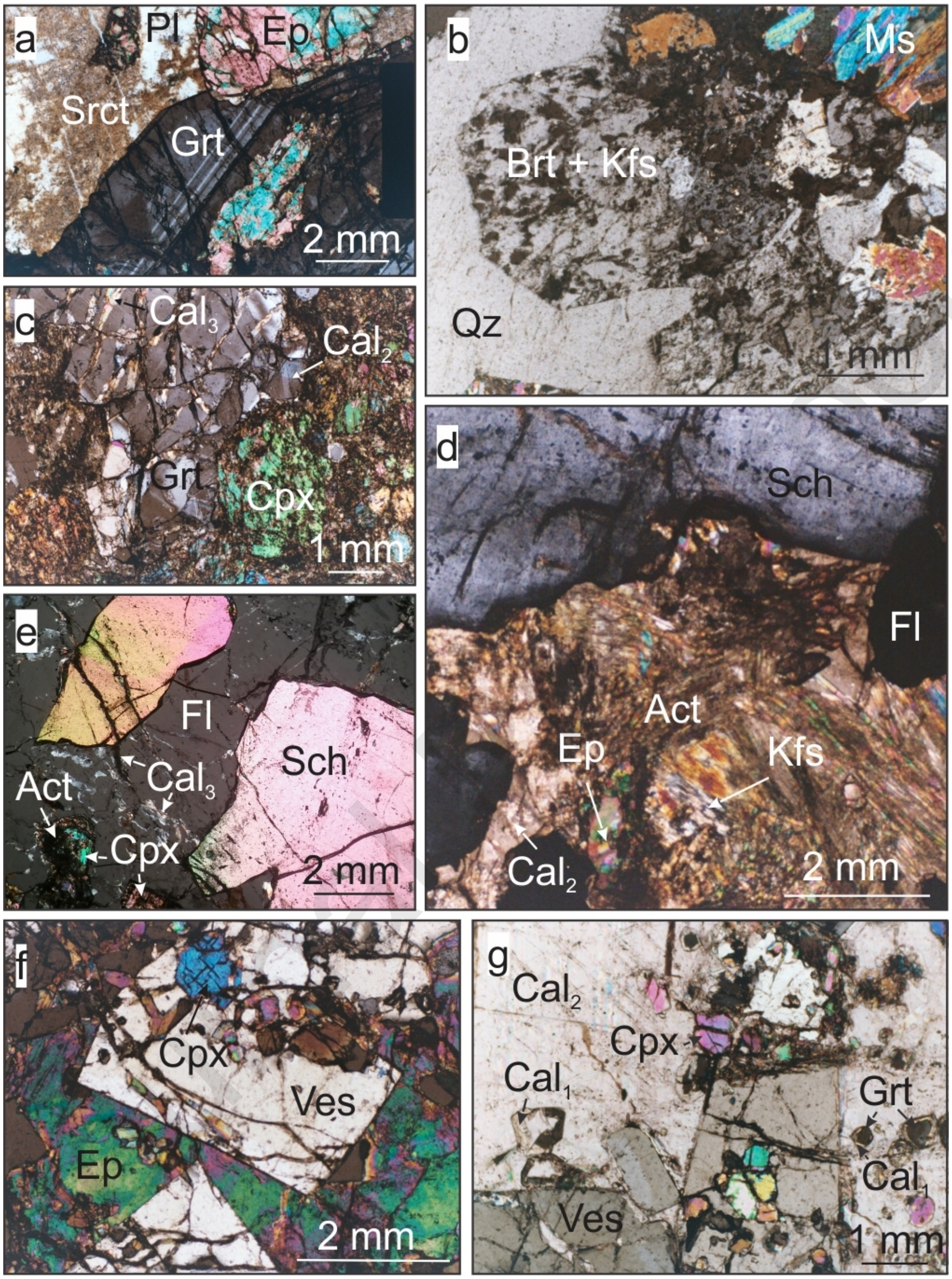
a
Pl
Ep
Srct
Grt
2 mm
b
Ms
Brt + Kfs
Qz
1 mm
c
Cal$_3$
Cal$_2$
Grt
Cpx
1 mm
d
Sch
Fl
Act
Ep
Kfs
Cal$_2$
2 mm
e
Fl
Sch
Act
Cal$_3$
Cpx
2 mm
f
Cpx
Ves
Ep
2 mm
g
Cal$_2$
Cpx
Cal$_1$
Grt
Cal$_1$
Ves
1 mm

1047 Figure 6

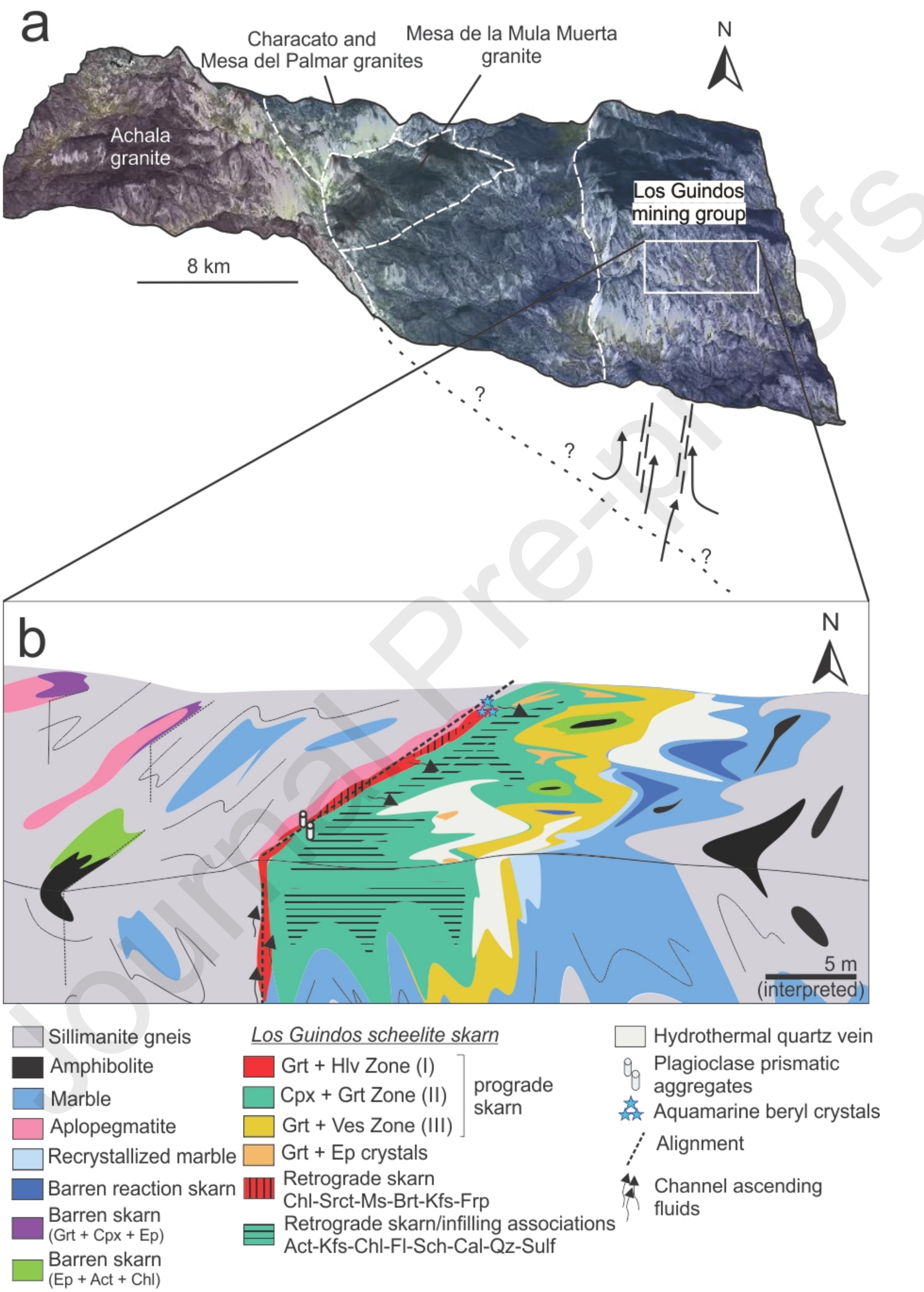

1048

Figure 7 (Espeche et al.)

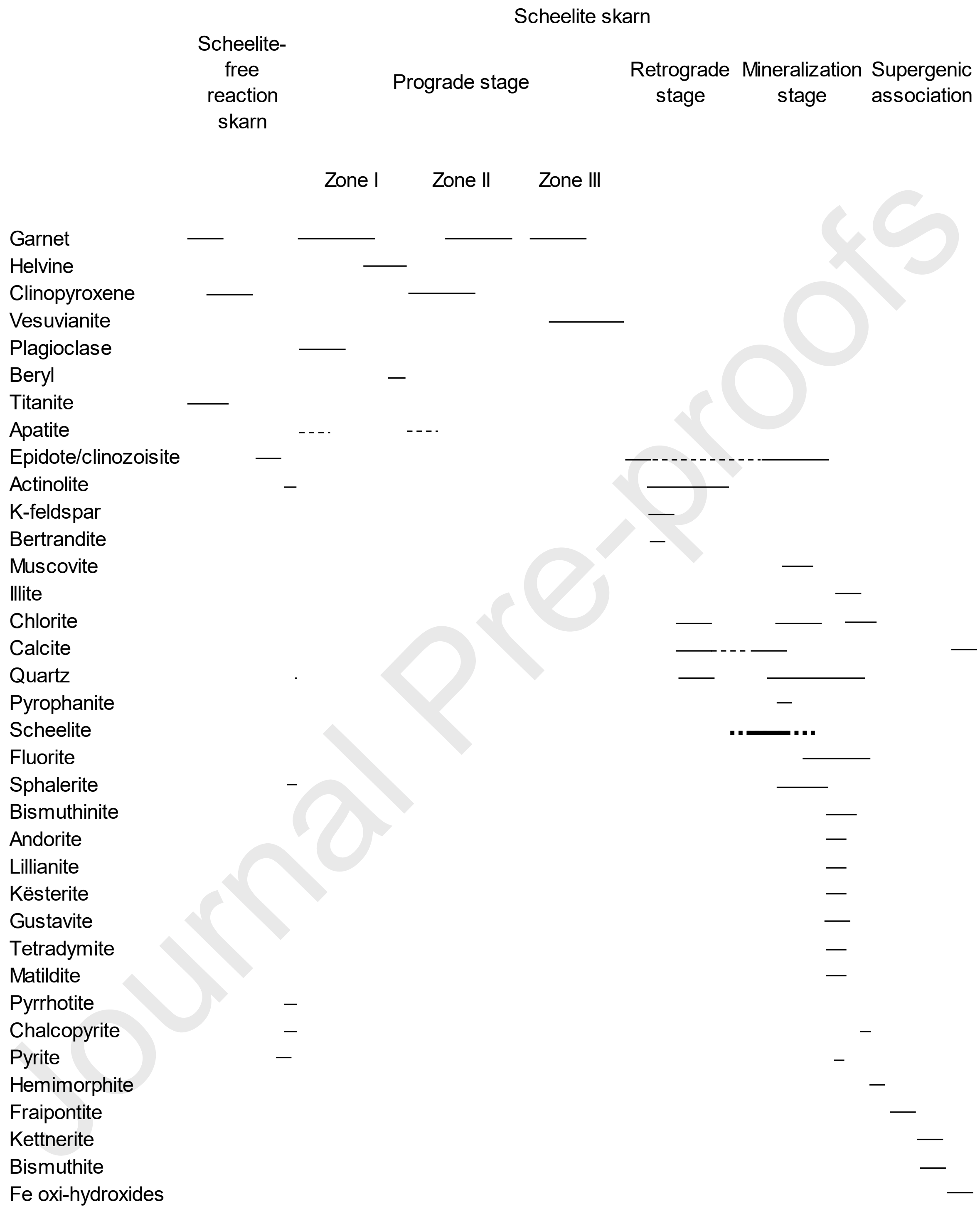

1054 Figure 8 (Espeche et al.)

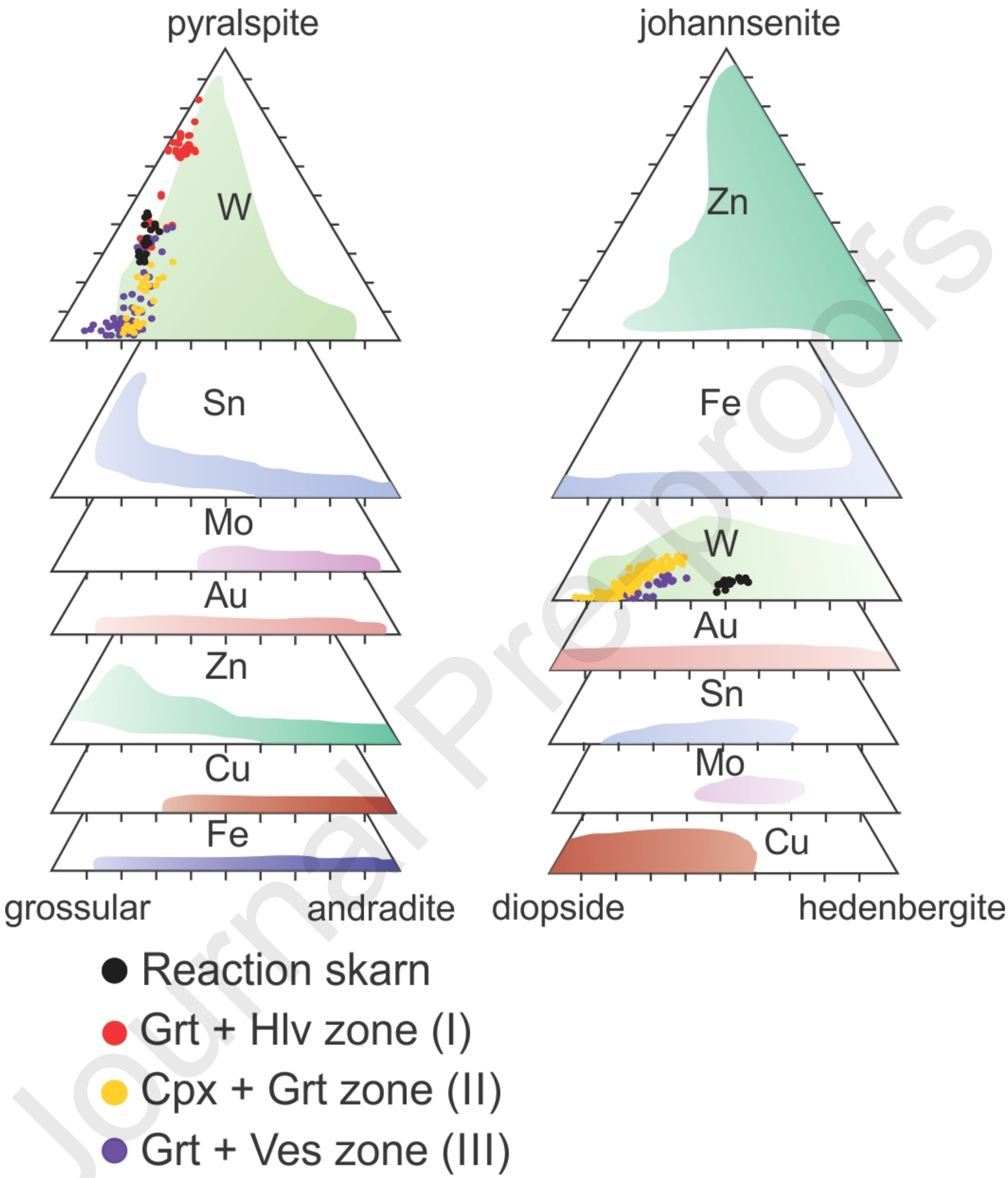

1055

1056

1057

1058

1059

1060 Figure 9 (Espeche et al.)

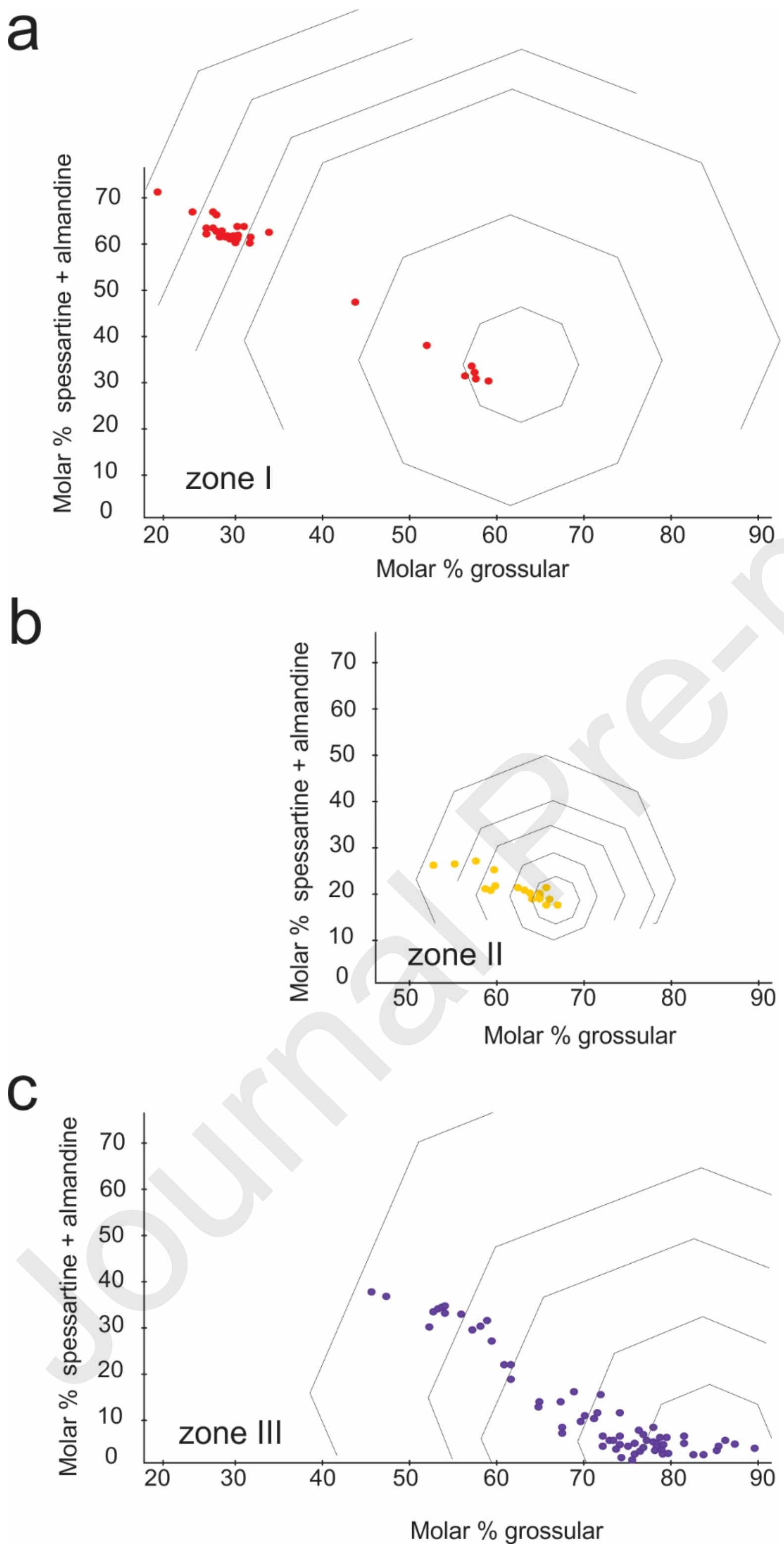

1061

1062

Figure 10 (Espeche et al.)

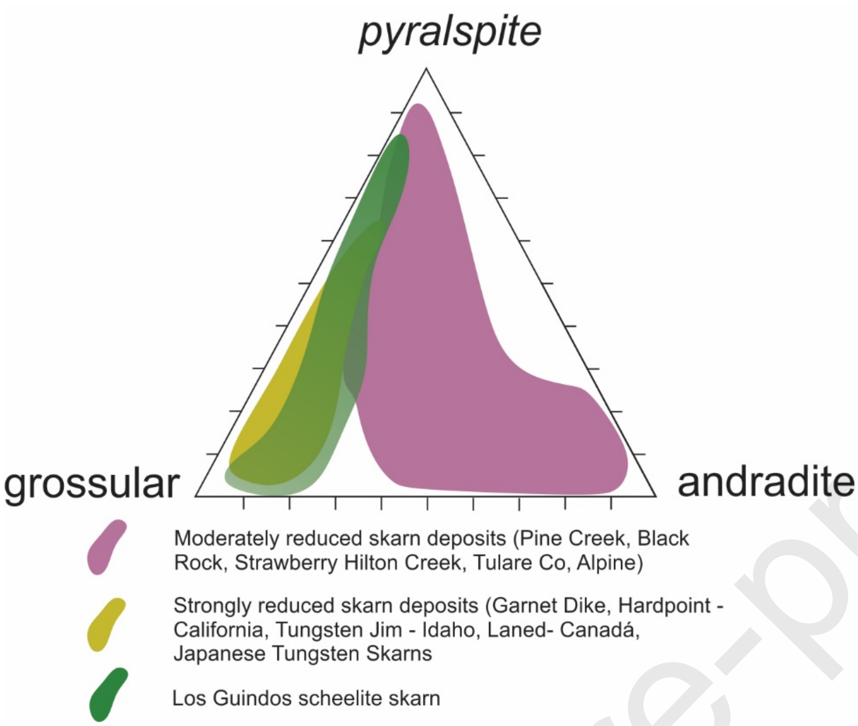

Figure 11 (Espeche et al.)

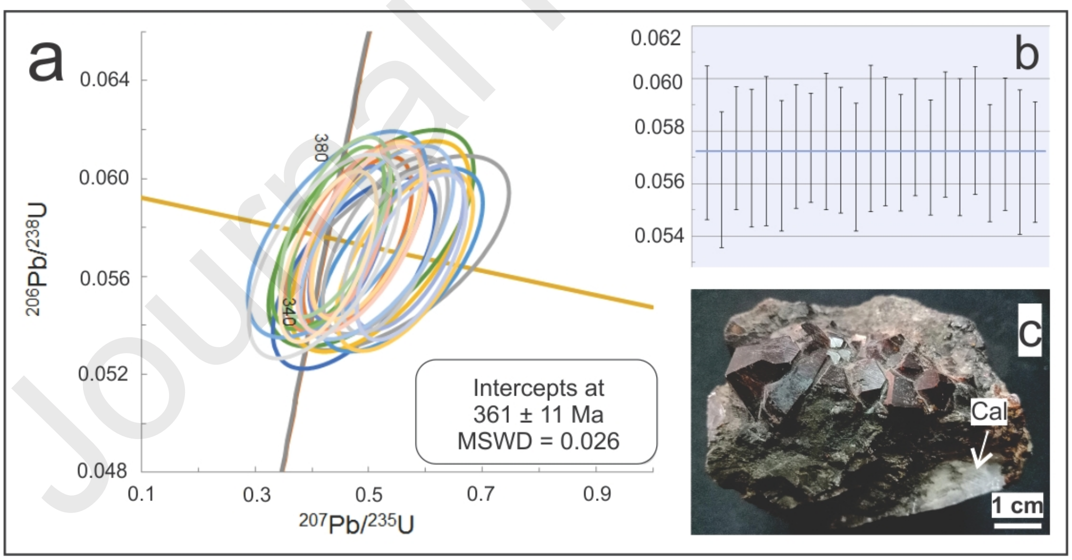

Figure 12 (Espeche et al.)

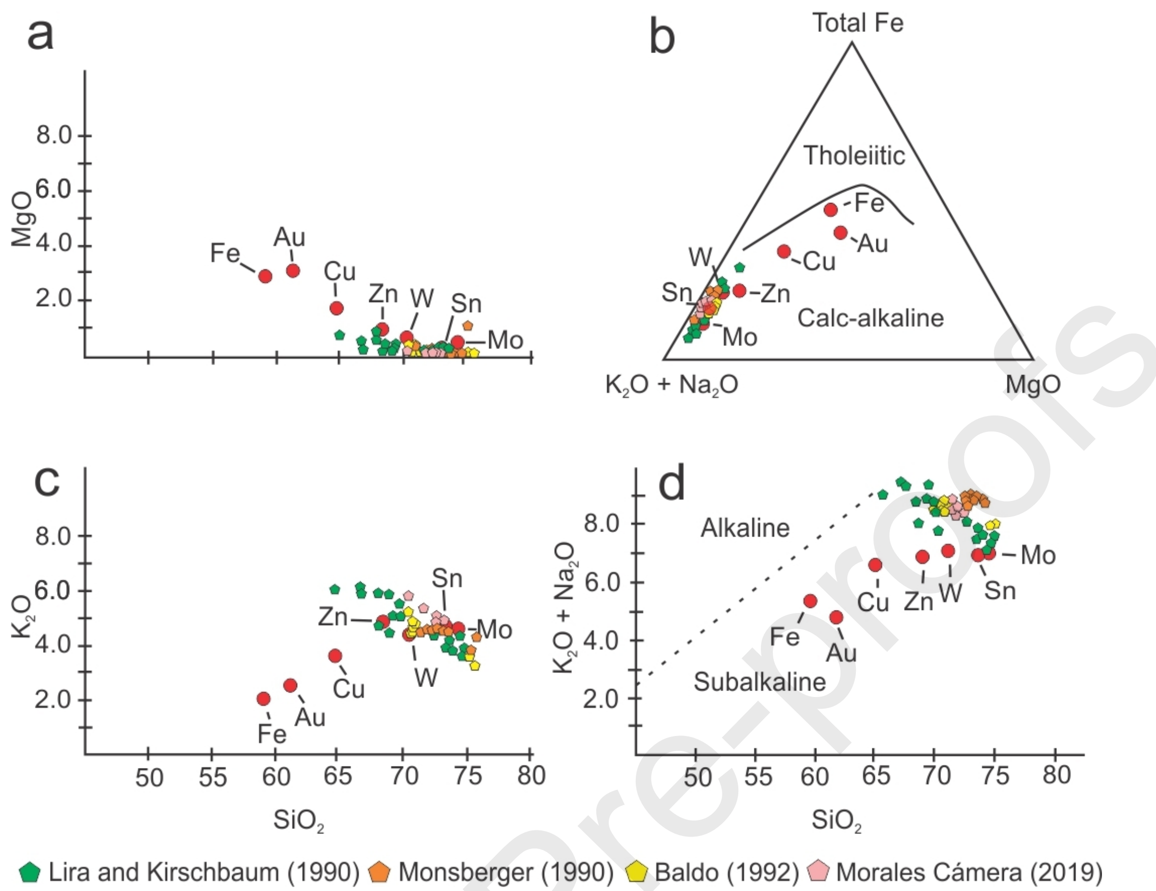

Figure 13

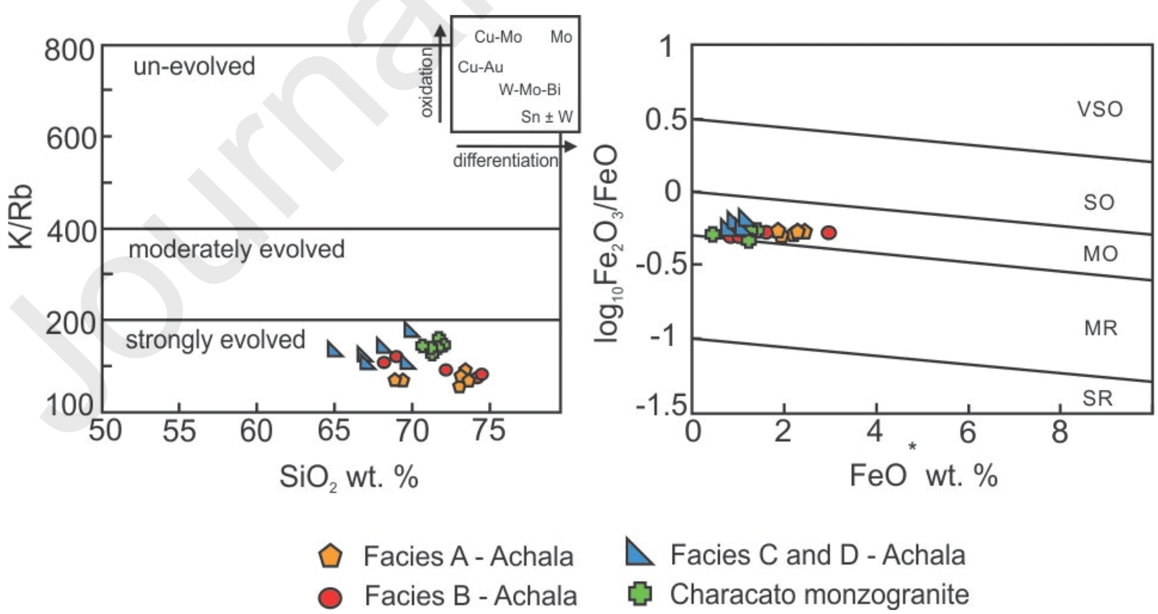

HIGHLIGHTS

- Los Guindos scheelite skarn deposit is one of the main W deposits in Pampean Ranges
- Mineral chemistry classified this skarn in the worldwide W skarn deposits
- U-Pb age on prograde garnet give an age of 361 ± 11 Ma.
- Isotopic age coincides with the final stages of crystallization of Achala magmatism
- Skarn related fluids are considered as magmatic-hydrothermal fluids of Devonian age